Model A-EE : An Eulerian Two-Phase Gas-Solid Model

Hudson, Justin and Harris, David

2006

MIMS EPrint: **2006.11**

Manchester Institute for Mathematical Sciences
School of Mathematics

The University of Manchester

ISSN 1749-9097

Model A-EE : An Eulerian Two-Phase Gas-Solid Model

Justin Hudson * David Harris†

Abstract

This paper investigates Model A (as discussed by Hudson & Harris [7]) with the inclusion of a gas Energy equation. We present two formulations of the model and discretise them using the Lax-Wendroff, MacCormack and a high resolution scheme. Three different test cases are used to compare the results to determine the accuracy and robustness of the schemes. The results of Model A-EE are also compared to the isentropic model (Model A).

1 Introduction

Hudson & Harris [7] presented a detailed discussion on two different two-phase models (usually denoted as Models A & B) for a gas-solid regime, which are well documented in the literature (see Jackson [8], Ding & Gidaspow [3], Lyczkowski [12] and Boemer *et al.* [2]). We extend one of the models (Model A) to include a gas Energy equation and discretise using three numerical schemes: Lax-Wendroff, MacCormack and a high resolution scheme. It is essential that the schemes are robust and produce an accurate approximation for a variety of test cases. Thus, we apply the schemes to a basic advection test case in order to determine the accuracy of the schemes. We also consider a pure gas test case in order to ensure that the numerical solution of the model is the same as the

*School of Mathematics, University of Manchester, Sackville Street, Manchester, M60 1QD (justin.hudson@manchester.ac.uk)

†School of Mathematics, University of Manchester, Sackville Street, Manchester, M60 1QD (david.harris@manchester.ac.uk)

standard Euler equations. A square pulse test case, which was discussed in Hudson & Harris [7], is also investigated to see if the numerical results are similar to the isentropic Model A.

2 Mathematical Formulation

2.1 Model A-EE

We now introduce Model A-EE, which for the gas phase consists of: the mass equation,

$$(\epsilon_g \rho_g)_t + (\epsilon_g \rho_g u_g)_x = 0, \tag{2.1}$$

the momentum equation

$$(\epsilon_g \rho_g u_g)_t + (\epsilon_g \rho_g u_g^2)_x + \epsilon_g (p_g)_x = -\beta(u_g - u_s) \tag{2.2}$$

and the Energy equation

$$(\epsilon_g E_g)_t + (\epsilon_g u_g (E_g + p_g))_x + p_g (\epsilon_s u_s)_x = -\beta u_g (u_g - u_s). \tag{2.3}$$

and for the solids phase: the mass equation,

$$(\rho_s \epsilon_s)_t + (\rho_s \epsilon_s u_s)_x = 0, \tag{2.4}$$

the momentum equation

$$(\rho_s \epsilon_s u_s)_t + (\epsilon_s \rho_s u_s^2)_x + \epsilon_s (p_g)_x + (p_s)_x = \beta(u_g - u_s) \tag{2.5}$$

and the fluctuating energy equation,

$$(\epsilon_s \rho_s T_s)_t + (\epsilon_s \rho_s u_s T_s)_x = -\frac{2}{3}\left(p_s (u_s)_x + 3\beta T_s\right). \tag{2.6}$$

Here, ρ_k is the density, u_k is the velocity, p_k is pressure, T_s is the granular temperature and the total energy per unit volume is

$$E_g = \left(e_g + \frac{1}{2}u_g^2\right)\rho_g,$$

where k denotes the gas (g) or solids (s) phase. The specific internal energy is e_g, which for ideal gases is

$$e_g = \frac{p_g}{(\gamma_g - 1)\rho_g} \quad \Rightarrow \quad p_g = (\gamma_g - 1)(E_g - \frac{1}{2}\rho_g u_g^2),$$

where γ_g denotes the ratio of specific heat capacities of the gas. The solids pressure is

$$p_s(\epsilon_s, T_s) = \epsilon_s \rho_s T_s.$$

and the drag force is

$$\beta = \frac{C_D}{d_s} \epsilon_g \epsilon_s \rho_g (u_g - u_s),$$

where C_D is a dimensionless parameter and d_s is the solids particle diameter. In order to close the model, we take the solids density ρ_s to be a constant.

2.2 Gas and Solids Data

We consider the case of glass beads being transported by air and take a solids density of $\rho_s = 2660$ kg/m^3 and particle diameter $d_s = 0.005$ m. For the gas phase, data corresponding to air at room temperature (20°C) with atmospheric pressure (100.0437 kPa), density $\rho_g = 1.2885$ kg/m^3, viscosity $\mu_g = 1.58 \times 10^{-7}$ Pa.s and $\gamma_g = 1.4$ are used.

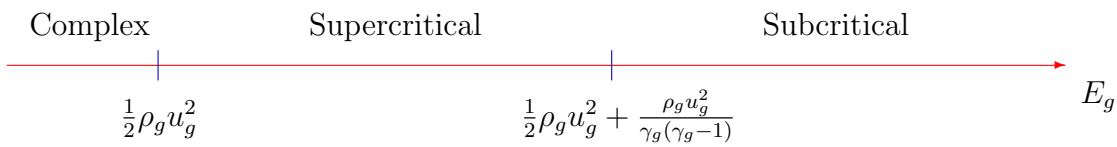

Figure 2.1: Gas Phase Flow Type.

Figure 2.1 illustrates the flow type of the gas phase, where

$$E_g \geq \frac{1}{2}\rho_g u_g^2,$$

otherwise two of the roots of the gas phase are complex. We are primarily interested in subcritical flow for the gas phase since the gas pressure is typically large for the regime under investigation.

3 Classification

In this section we consider whether each model is hyperbolic for the regime under investigation, both for the suitability of the scheme and for the implementation of the initial and

boundary conditions for the test cases. We intend to solve the equations only in regimes where the equations are hyperbolic and need to investigate when this is the case.

A system of partial differential equations is hyperbolic if the physical wave speeds (obtained from the canonical form) of the system are all real and there exists a complete set of linearly independent eigenvectors, see LeVeque [10]. A full set of linearly independent eigenvectors can be found for both models thus, we must ensure that the wave speeds are all real.

We can rewrite Model A-EE in canonical form (see Appendix A) as

$$\begin{bmatrix} \rho_g \\ u_g \\ p_g \\ \epsilon_s \\ u_s \\ T_s \end{bmatrix}_t + \begin{bmatrix} u_g & \rho_g & 0 & \frac{\rho_g}{\epsilon_g}(u_s - u_g) & \frac{\rho_g \epsilon_s}{\epsilon_g} & 0 \\ 0 & u_g & \rho_g^{-1} & 0 & 0 & 0 \\ 0 & \gamma p_g & u_g & \frac{\gamma p_g}{\epsilon_g}(u_s - u_g) & \frac{\gamma p_g \epsilon_s}{\epsilon_g} & 0 \\ 0 & 0 & 0 & u_s & \epsilon_s & 0 \\ 0 & 0 & {\rho_s}^{-1} & \frac{T_s}{\epsilon_s} & u_s & 1 \\ 0 & 0 & 0 & 0 & \frac{2}{3}T_s & u_s \end{bmatrix} \begin{bmatrix} \rho_g \\ u_g \\ p_g \\ \epsilon_s \\ u_s \\ T_s \end{bmatrix}_x = \begin{bmatrix} 0 \\ -\frac{\beta}{\epsilon_g \rho_g}(u_g - u_s) \\ -\frac{(\gamma-1)\beta}{\epsilon_g}(u_g - u_s)^2 \\ 0 \\ \frac{\beta}{\rho_s \epsilon_s}(u_g - u_s) \\ -\frac{2\beta}{\rho_s \epsilon_s}T_s \end{bmatrix}.$$

The characteristic equation of this system is,

$$|\mathbf{A} - \lambda \mathbf{I}| = (\lambda - u_s)(\lambda - u_g)(a_4\lambda^4 + a_3\lambda^3 + a_2\lambda^2 + a_1\lambda + a_0) = 0,$$

where

$$a_4 = 3\rho_s\rho_g\epsilon_g, \quad a_3 = -6\rho_s\rho_g\epsilon_g(u_g + u_s),$$
$$a_2 = -3\gamma p_g(\epsilon_g\rho_s + \rho_g\epsilon_s) - 5\rho_g\rho_s\epsilon_g T_s + 3\rho_s\rho_g\epsilon_g(u_s^2 + u_g^2 + 4u_g u_s),$$
$$a_1 = 6p_g\gamma(\epsilon_g\rho_s u_s + \epsilon_s\rho_g u_g) + 10\rho_g\rho_s\epsilon_g u_g T_s - 6\rho_g\rho_s\epsilon_g u_g u_s(u_s + u_g)$$

and

$$a_0 = -3p_g\gamma(\epsilon_g\rho_s u_s^2 + \epsilon_s\rho_g u_g^2) + 5\epsilon_g T_s\rho_s(\gamma p_g - \rho_g u_g^2) + 3\rho_s\rho_g\epsilon_g u_g^2 u_s^2.$$

Thus, two of the eigenvalues are always real and the other four are determined by solving the quartic. Unfortunately, the roots of this quartic can in general not be found analytically. Thus, we use Matlab to determine the roots numerically. We use the constant values in Section 2.2 and then solve the quartic for a variety of values of the remaining variables appearing in the coefficients a_k. The Matlab program calculates the values of a_k, calculates the roots numerically using the built in command c=roots(a_k) and determines if any root is complex by using the command image(c), with image(c)$\neq$ 0 if a root is complex.

Figures 3.1 and 3.2 illustrate various contour plots for certain fixed values of ϵ_s, ρ_g and T_s to show combinations of values resulting in complex roots. Here, we can see that when

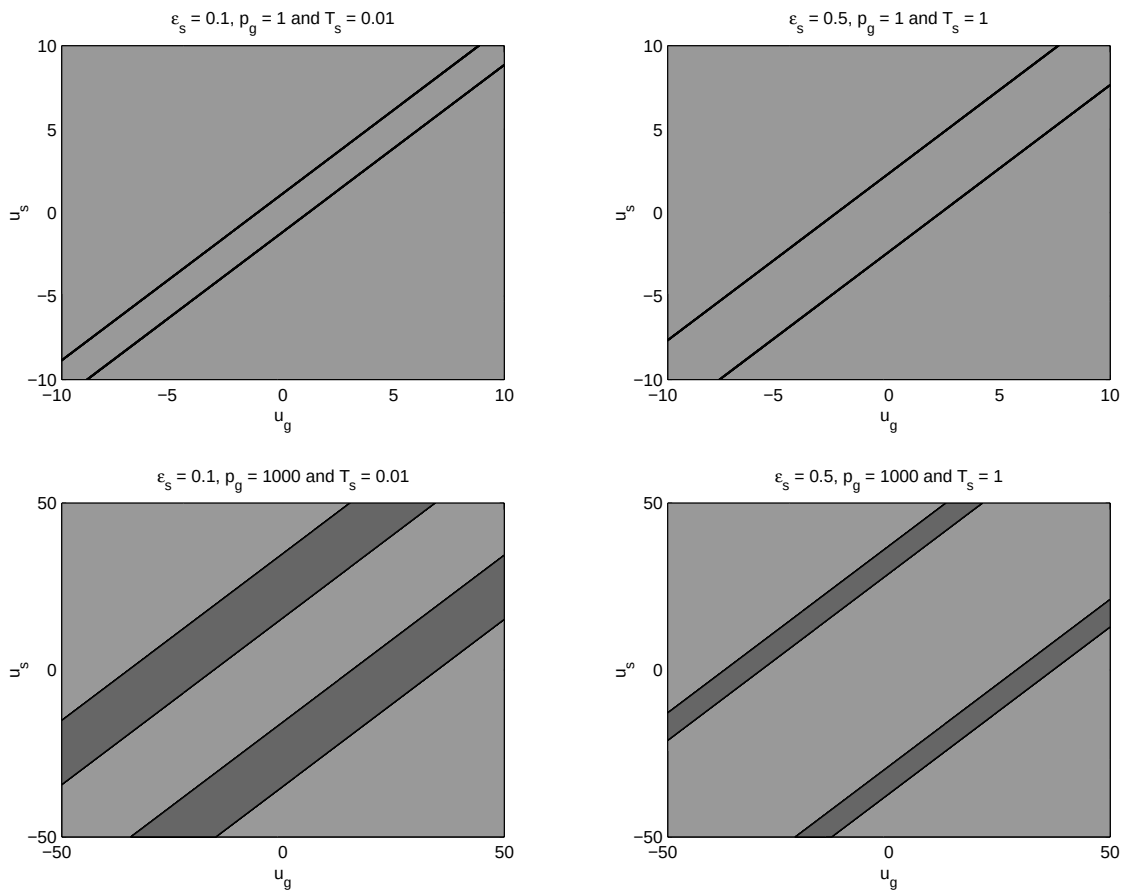

Figure 3.1: Model A with constant gas pressure.

the gas pressure is constant, two regions of real roots exist that are dependent on $u_g - u_s$. As p_g increases, the region of complex roots increases and the first interval of real roots around $u_k = 0$ expands in size. If T_s is increased, the region of complex roots is reduced in size. When the gas pressure is not constant, the dependence on $u_g - u_s$ is significantly reduced and an elliptic area of complex roots is produced. For small values of E_g and large values of T_s, the region of complex roots is small. Thus, Model A-EE is only conditionally hyperbolic.

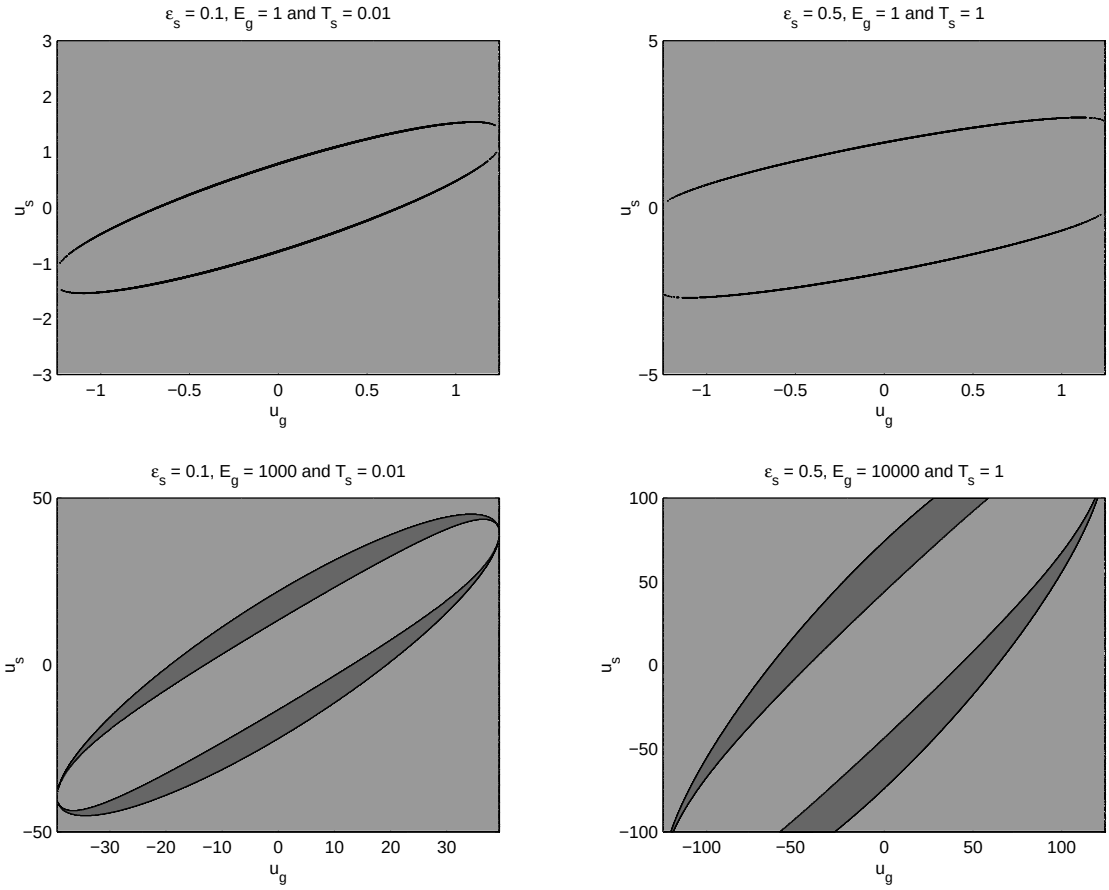

Figure 3.2: Model A without constant gas pressure ($|u_g| \geq \sqrt{\frac{2E_g}{\rho_g}}$).

4 Formulations

In order to help maximise the accuracy of the schemes which are presented in Section 5, we present two different formulations of Model A-EE. Each is written in conservative variable form to ensure that shocks propagate at the correct speed and comprises a system of inhomogeneous conservation laws which may be written as

$$\mathbf{w}_t + \mathbf{F}(\mathbf{w})_x = \mathbf{R} + \mathbf{S}, \tag{4.1}$$

where $\mathbf{F}(\mathbf{w})$ denotes the flux-function, $\mathbf{R}$ denotes the inhomogeneous terms which contain spatial derivatives of the dependent variables and $\mathbf{S}$ denotes the remaining inhomogeneous terms without such derivatives. The inhomogeneous terms are split in this manner to aid the numerical discretisation presented in the next section.

4.1 Formulation AES

The first formulation is obtained by using the product rule,

$$(\epsilon_g p_g)_x = \epsilon_g (p_g)_x + p_g (\epsilon_g)_x,$$

thus,

$$\begin{bmatrix} \epsilon_g \rho_g \\ \epsilon_g \rho_g u_g \\ \epsilon_g E_g \\ \epsilon_s \\ \epsilon_s u_s \\ \epsilon_s T_s \end{bmatrix}_t + \begin{bmatrix} \epsilon_g \rho_g u_g \\ \epsilon_g \rho_g u_g^2 + \epsilon_g p_g \\ \epsilon_g u_g (E_g + p_g) \\ \epsilon_s u_s \\ \epsilon_s u_s^2 + \epsilon_s T_s \\ \epsilon_s u_s T_s \end{bmatrix}_x = \begin{bmatrix} 0 \\ p_g (\epsilon_g)_x \\ -p_g (\epsilon_s u_s)_x \\ 0 \\ -\rho_s^{-1} \epsilon_s (p_g)_x \\ -\frac{2}{3} \epsilon_s T_s (u_s)_x \end{bmatrix} + \begin{bmatrix} 0 \\ -\beta (u_g - u_s) \\ -\beta u_s (u_g - u_s) \\ 0 \\ \rho_s^{-1} \beta (u_g - u_s) \\ -2 \rho_s^{-1} \beta T_s \end{bmatrix}. \tag{4.2}$$

The Jacobian matrix is

$$\mathbf{A} = \begin{bmatrix} \mathbf{A}_g & 0 \\ 0 & \mathbf{A}_s \end{bmatrix},$$

where

$$\mathbf{A}_g = \begin{bmatrix} 0 & 1 & 0 \\ \frac{1}{2}(\gamma_g - 3) u_g^2 & (3 - \gamma_g) u_g & (\gamma_g - 1) \\ u_g (\frac{1}{2}(\gamma_g - 1) u_g^2 - H_g) & H_g - (\gamma_g - 1) u_g^2 & \gamma_g u_g \end{bmatrix}$$

and

$$\mathbf{A}_s = \begin{bmatrix} 0 & 1 & 0 \\ -u_s^2 & 2 u_s & 1 \\ -u_s T_s & T_s & u_s \end{bmatrix}.$$

The total specific enthalpy is

$$H_g = \frac{E_g + p_g}{\rho_g} = \frac{c_g^2}{\gamma_g - 1} + \frac{1}{2} u_g^2$$

and the sound speed (of the gas phase) is

$$c_g = \sqrt{\frac{\gamma_g p_g}{\rho_g}} = \sqrt{\frac{\gamma_g}{\rho_g} (\gamma_g - 1)(E_g - \frac{1}{2} \rho_g u_g^2)}.$$

Since the Jacobian is block diagonal, we can discretise the two phases separately, which significantly reduces the complexity of the numerics.

4.2 Formulation AEP

The term $p_s(u_s)_x$, which is present in the fluctuation energy equation can create numerical difficulties. In order to try and rectify this problem, we use the product rule to split this term,

$$\begin{bmatrix} \epsilon_g\rho_g \\ \epsilon_g\rho_g u_g \\ \epsilon_g E_g \\ \epsilon_s \\ \epsilon_s u_s \\ \epsilon_s T_s \end{bmatrix}_t + \begin{bmatrix} \epsilon_g\rho_g u_g \\ \epsilon_g\rho_g u_g^2 + \epsilon_g p_g \\ \epsilon_g u_g(E_g + p_g) \\ \epsilon_s u_s \\ \epsilon_s u_s^2 + \epsilon_s T_s \\ \frac{5}{3}\epsilon_s u_s T_s \end{bmatrix}_x = \begin{bmatrix} 0 \\ p_g(\epsilon_g)_x \\ -p_g(\epsilon_s u_s)_x \\ 0 \\ -\rho_s^{-1}\epsilon_s(p_g)_x \\ \frac{2}{3}u_s(\epsilon_s T_s)_x \end{bmatrix} + \begin{bmatrix} 0 \\ -\beta(u_g - u_s) \\ -\beta u_s(u_g - u_s) \\ 0 \\ \rho_s^{-1}\beta(u_g - u_s) \\ -2\rho_s^{-1}\beta T_s \end{bmatrix}. \tag{4.3}$$

As with Formulation AES, the Jacobian is block diagonal, but with a different solids Jacobian,

$$\mathbf{A}_s = \begin{bmatrix} 0 & 1 & 0 \\ -u_s^2 & 2u_s & 1 \\ -\frac{5}{3}u_s T_s & \frac{5}{3}T_s & \frac{5}{3}u_s \end{bmatrix}.$$

5 Numerical Schemes

We now introduce a variety of numerical schemes, which can be used to approximate the different formulations. To ensure the schemes remains stable, the time step is calculated using

$$\Delta t = \frac{\nu \Delta x}{\max(|\lambda|)},$$

where $\max(|\lambda|)$ is the maximum wave speed and $\nu \leq 1$ is the required Courant number.

In order to test the robustness and accuracy of the different schemes, we consider a simple advection test case,

$$\epsilon_s(x,t) = \epsilon_s^0(x - Ut, 0), \quad u_g(x,t) = u_s(x,t) = U, \quad \rho_g(x,t) = R,$$

$$E_g(x,t) = E \quad \text{and} \quad T_s(x,t) = \frac{P_s}{\epsilon_s},$$

where R, U, E and P_s are all constants. We expect a numerical scheme to be exact when $U = 0$ and preserve the constants for any value of U.

Throughout this section, we use the definitions:

$$\Delta^F a = a_{i+1} - a_i, \quad \Delta^C a = a_{i+1} - a_{i-1}, \quad \Delta^B a = a_i - a_{i-1}$$

and

$$\Delta^2 a = a_{i+1} - 2a_i + a_{i-1}.$$

5.1 Lax-Wendroff Scheme

The first scheme we consider is the adapted Lax-Wendroff scheme with second order source term approximation [6]:

$$\begin{aligned}\mathbf{w}_i^{n+1} = \mathbf{w}_i^n &- \frac{s}{2}(\mathbf{F}_{i+1}^n - \mathbf{F}_{i-1}^n) + \frac{s}{2}(\mathbf{R}_{i+\frac{1}{2}}^n + \mathbf{R}_{i-\frac{1}{2}}^n) + \Delta t \mathbf{S}_i^n \\ &+ \frac{s^2}{2}\left(\mathbf{A}_{i+\frac{1}{2}}(\mathbf{F}_{i+1}^n - \mathbf{F}_i^n) - \mathbf{A}_{i-\frac{1}{2}}(\mathbf{F}_i^n - \mathbf{F}_{i-1}^n)\right) - \frac{s^2}{2}\left(\mathbf{A}_{i+\frac{1}{2}}\mathbf{R}_{i+\frac{1}{2}} - \mathbf{A}_{i-\frac{1}{2}}\mathbf{R}_{i-\frac{1}{2}}\right).\end{aligned}$$

Here, the Jacobians are approximated using the standard average approach,

$$\mathbf{A}_{i+\frac{1}{2}} = \mathbf{A}(\hat{\mathbf{w}}_{i+\frac{1}{2}}) \quad \text{where} \quad \hat{\mathbf{w}}_{i+\frac{1}{2}} = \frac{1}{2}(\mathbf{w}_{i+1}^n + \mathbf{w}_i^n)$$

and the source term approximations are

$$\mathbf{R}_{i+\frac{1}{2}}^n = \begin{bmatrix} 0 \\ \hat{p_g}\Delta^F \epsilon_g \\ -\hat{p_g}\Delta^F(\epsilon_s u_s) \\ 0 \\ -\rho_s^{-1}\hat{\epsilon_s}\Delta^F p_g \\ r_6 \end{bmatrix}_i^n \quad \text{and} \quad \mathbf{S}_i^n = \begin{bmatrix} 0 \\ -\beta(u_g - u_s) \\ -\beta u_s(u_g - u_s) \\ 0 \\ \rho_s^{-1}\beta(u_g - u_s) \\ -2\rho_s^{-1}\beta T_s \end{bmatrix}_i^n,$$

where

$$r_6 = -\frac{2}{3}\hat{\epsilon_s}\hat{T_s}\Delta^F u_s$$

for Formulation AES,

$$r_6 = \frac{2}{3}\hat{u_s}\Delta^F(\epsilon_s T_s)$$

for Formulation AEP and $\hat{a} = \frac{1}{2}(a_{i+1} + a_i)$.

5.1.1 Accuracy for Advection Test Case

We consider the accuracy of the scheme for Formulation AES when approximating the advection test case:

$$
\begin{bmatrix} R\epsilon_g \\ RU\epsilon_g \\ E\epsilon_g \\ \epsilon_s \\ U\epsilon_s \\ P_s \end{bmatrix}_i^{n+1} = \begin{bmatrix} R\epsilon_g \\ RU\epsilon_g \\ E\epsilon_g \\ \epsilon_s \\ U\epsilon_s \\ P_s \end{bmatrix}_i^{n} - \frac{s}{2}\left(\begin{bmatrix} RU\epsilon_g \\ (RU^2+P_g)\epsilon_g \\ U(E+P_g)\epsilon_g \\ U\epsilon_s \\ U^2\epsilon_s + P_s \\ UP_s \end{bmatrix}_{i+1}^{n} - \begin{bmatrix} RU\epsilon_g \\ (RU^2+P_g)\epsilon_g \\ U(E+P_g)\epsilon_g \\ U\epsilon_s \\ U^2\epsilon_s + P_s \\ UP_s \end{bmatrix}_{i-1}^{n} \right)
$$

$$
+ \frac{s^2}{2} \begin{bmatrix} (RU^2+P_g)\Delta^2\epsilon_g \\ (\frac{1}{2}(\gamma_g-3)RU^3 + (3-\gamma_g)U(RU^2+P_g) + (\gamma_g-1)U(E+P_g))\Delta^2\epsilon_g \\ (RU^2(\frac{1}{2}(\gamma_g-1)U^2 - H) + (H-(\gamma_g-1)U^2)(RU^2+P_g) + U^2(E+P_g)\gamma_g)\Delta^2\epsilon_g \\ U^2\Delta^2\epsilon_s \\ (-U^3+2U^3)\Delta^2\epsilon_s \\ (-U^2T_s + T_sU^2)\Delta^2\epsilon_s \end{bmatrix}
$$

$$
- \frac{s^2}{2} \begin{bmatrix} P_g\Delta^2\epsilon_g \\ ((3-\gamma_g)UP_g + (\gamma_g-1)P_gU)\Delta^2\epsilon_g \\ ((H-(\gamma_g-1)U^2)P_g + \gamma_gU^2P_g\ )\Delta^2\epsilon_g \\ 0 \\ 0 \\ 0 \end{bmatrix} + \frac{s}{2} \begin{bmatrix} 0 \\ P_g(\Delta^F\epsilon_g + \Delta^B\epsilon_g) \\ -P_gU(\Delta^F\epsilon_s + \Delta^B\epsilon_s) \\ 0 \\ 0 \\ 0 \end{bmatrix}.
$$

Simplifying

$$
\frac{1}{2}(\gamma_g-3)RU^3 + (3-\gamma_g)U(RU^2+P_g) + (\gamma_g-1)U(E+P_g)
$$

$$
\Rightarrow \quad -\frac{1}{2}(\gamma_G-3)RU^3 + (3-\gamma_g)UP_g + (\gamma_g-1)U(E+P_g)
$$

$$
\Rightarrow \quad -\frac{1}{2}(\gamma_G-3)RU^3 + 2UP_g + +(\gamma_g-1)UE
$$

$$
\Rightarrow \quad RU^3 + 2UP_g + +(\gamma_g-1)U(E - \frac{1}{2}RU^2)
$$

$$
\Rightarrow \quad RU^3 + 3UP_g
$$

and

$$
RU^2(\frac{1}{2}(\gamma_g-1)U^2 - H) + (H-(\gamma_g-1)U^2)(RU^2+P_g) + U^2(E+P_g)\gamma_g
$$

$$
\Rightarrow \quad -\frac{1}{2}RU^4(\gamma_g-1) + P_gH - (\gamma_g-1)U^2P_g + U^2(E+P_g)\gamma_g
$$

$$\Rightarrow \quad (\gamma_g - 1)U^2(E - \frac{1}{2}RU^2) + P_g H + U^2 P_g + U^2 E$$
$$\Rightarrow \quad P_g H + 2U^2 P_g + U^2 E.$$

Thus,

$$\begin{bmatrix} R\epsilon_g \\ RU\epsilon_g \\ E\epsilon_g \\ \epsilon_s \\ U\epsilon_s \\ P_s \end{bmatrix}_i^{n+1} = \begin{bmatrix} R\epsilon_g \\ RU\epsilon_g \\ E\epsilon_g \\ \epsilon_s \\ U\epsilon_s \\ P_s \end{bmatrix}_i^{n} - \frac{s}{2}\begin{bmatrix} RU\Delta^C\epsilon_g \\ RU^2\Delta^C\epsilon_g \\ UE\Delta^C\epsilon_g \\ U\Delta^C\epsilon_s \\ U^2\Delta^C\epsilon_s \\ 0 \end{bmatrix}$$
$$+ \frac{s^2}{2}\begin{bmatrix} (RU^2 + P_g)\Delta^2\epsilon_g \\ (RU^3 + 3UP_g)\Delta^2\epsilon_g \\ (P_g H + 2U^2 P_g + U^2 E)\Delta^2\epsilon_g \\ U^2\Delta^2\epsilon_s \\ U^3\Delta^2\epsilon_s \\ 0 \end{bmatrix} - \frac{s^2}{2}\begin{bmatrix} P_g\Delta^2\epsilon_g \\ 2UP_g\Delta^2\epsilon_g \\ (HP_g + U^2 P_g)\Delta^2\epsilon_g \\ 0 \\ 0 \\ 0 \end{bmatrix}.$$

Hence,

$$\begin{bmatrix} R\epsilon_g \\ RU\epsilon_g \\ E\epsilon_g \\ \epsilon_s \\ U\epsilon_s \\ P_s \end{bmatrix}_i^{n+1} = \begin{bmatrix} R\epsilon_g \\ RU\epsilon_g \\ E\epsilon_g \\ \epsilon_s \\ U\epsilon_s \\ P_s \end{bmatrix}_i^{n} - \frac{s}{2}\begin{bmatrix} RU\Delta^C\epsilon_g \\ RU^2\Delta^C\epsilon_g \\ UE\Delta^C\epsilon_g \\ U\Delta^C\epsilon_s \\ U^2\Delta^C\epsilon_s \\ 0 \end{bmatrix} + \frac{s^2}{2}\begin{bmatrix} RU^2\Delta^2\epsilon_g \\ (RU^3 + UP_g)\Delta^2\epsilon_g \\ (U^2 P_g + U^2 E)\Delta^2\epsilon_g \\ U^2\Delta^2\epsilon_s \\ U^3\Delta^2\epsilon_s \\ 0 \end{bmatrix}.$$

Here, we can see that the second and third equations are not consistent. Thus, surprisingly this scheme may produce inaccurate results. However, notice that when $U = 0$, the scheme exactly preserves the steady state solution.

5.2 MacCormack Approach

We consider the adapted MacCormack approach as discussed by LeVeque & Yee [11],

$$\mathbf{w}_i^{n+1} = \frac{1}{2}(\mathbf{w}_i^n + \mathbf{w}_i^{(1)}) - \frac{s}{2}(\mathbf{F}_i^{(1)} - \mathbf{F}_{i-1}^{(1)}) + \frac{s}{2}\mathbf{R}_{i-\frac{1}{2}}^{(1)} + \frac{\Delta t}{2}\mathbf{S}_{i-\frac{1}{2}}^{(1)},$$

where

$$\mathbf{w}_i^{(1)} = \mathbf{w}_i^n - s(\mathbf{F}_{i+1}^n - \mathbf{F}_i^n) + s\mathbf{R}_{i+\frac{1}{2}}^n + \Delta t\mathbf{S}_{i+\frac{1}{2}}^n.$$

Here, the source term approximations are

$$\mathbf{R}^n_{i+\frac{1}{2}} = \begin{bmatrix} 0 \\ \hat{p}_g \Delta^F \epsilon_g \\ -\hat{p}_g \Delta^F (\epsilon_s u_s) \\ 0 \\ -\rho_s^{-1} \hat{\epsilon}_s \Delta^F p_g \\ r_6 \end{bmatrix}^n_i \quad \text{and} \quad \mathbf{S}^n_{i+\frac{1}{2}} = \mathbf{S}(\hat{\mathbf{w}}^n_{i+\frac{1}{2}}),$$

where

$$r_6 = -\frac{2}{3} \hat{\epsilon}_s \hat{T}_s \Delta^F u_s$$

for Formulation AES,

$$r_6 = \frac{2}{3} \hat{u}_s \Delta^F (\epsilon_s T_s)$$

for Formulation AEP and $\hat{a} = \frac{1}{2}(a_{i+1} + a_i)$.

5.2.1 Accuracy for Advection Test Case

For the advection test case, MacCormack's scheme is (when approximating Formulation AES):

$$\begin{bmatrix} R\epsilon_g \\ RU\epsilon_g \\ E\epsilon_g \\ \epsilon_s \\ U\epsilon_s \\ P_s \end{bmatrix}^{(1)}_i = \begin{bmatrix} R\epsilon_g \\ RU\epsilon_g \\ E\epsilon_g \\ \epsilon_s \\ U\epsilon_s \\ P_s \end{bmatrix}^n_i - s \begin{bmatrix} RU\Delta^F \epsilon_g \\ (RU^2 + P_g)\Delta^F \epsilon_g \\ U(E + P_g)\Delta^F \epsilon_g \\ U\Delta^F \epsilon_s \\ U^2 \Delta^F \epsilon_s \\ 0 \end{bmatrix} + s \begin{bmatrix} 0 \\ P_g \Delta^F \epsilon_g \\ -P_g U \Delta^F \epsilon_s \\ 0 \\ 0 \\ 0 \end{bmatrix}$$

$$\Rightarrow \quad \begin{bmatrix} R\epsilon_g \\ RU\epsilon_g \\ E\epsilon_g \\ \epsilon_s \\ U\epsilon_s \\ P_s \end{bmatrix}^{(1)}_i = \begin{bmatrix} R\epsilon_g \\ RU\epsilon_g \\ E\epsilon_g \\ \epsilon_s \\ U\epsilon_s \\ P_s \end{bmatrix}^n_i - s \begin{bmatrix} RU\Delta^F \epsilon_g \\ RU^2 \Delta^F \epsilon_g \\ UE\Delta^F \epsilon_g \\ U\Delta^F \epsilon_s \\ U^2 \Delta^F \epsilon_s \\ 0 \end{bmatrix}$$

and

$$\begin{bmatrix} R\epsilon_g \\ RU\epsilon_g \\ E\epsilon_g \\ \epsilon_s \\ U\epsilon_s \\ P_s \end{bmatrix}_i^{n+1} = \frac{1}{2}\left(\begin{bmatrix} R\epsilon_g \\ RU\epsilon_g \\ E\epsilon_g \\ \epsilon_s \\ U\epsilon_s \\ P_s \end{bmatrix}_i^{n} + \begin{bmatrix} R\epsilon_g \\ RU\epsilon_g \\ E\epsilon_g \\ \epsilon_s \\ U\epsilon_s \\ P_s \end{bmatrix}_i^{(1)}\right) - \frac{s}{2}\begin{bmatrix} RU\Delta^B\epsilon_g \\ RU^2\Delta^B\epsilon_g \\ UE\Delta^B\epsilon_g \\ U\Delta^B\epsilon_s \\ U^2\Delta^B\epsilon_s \\ 0 \end{bmatrix}^{(1)}.$$

By substituting,

$$\begin{bmatrix} R\epsilon_g \\ RU\epsilon_g \\ E\epsilon_g \\ \epsilon_s \\ U\epsilon_s \\ P_s \end{bmatrix}_i^{n+1} = \begin{bmatrix} R\epsilon_g \\ RU\epsilon_g \\ E\epsilon_g \\ \epsilon_s \\ U\epsilon_s \\ P_s \end{bmatrix}_i^{n} - \frac{s}{2}\begin{bmatrix} RU\Delta^F\epsilon_g \\ RU^2\Delta^F\epsilon_g \\ UE\Delta^F\epsilon_g \\ U\Delta^F\epsilon_s \\ U^2\Delta^F\epsilon_s \\ 0 \end{bmatrix} - \frac{s}{2}\begin{bmatrix} RU\Delta^B\epsilon_g \\ RU^2\Delta^B\epsilon_g \\ UE\Delta^B\epsilon_g \\ U\Delta^B\epsilon_s \\ U^2\Delta^B\epsilon_s \\ 0 \end{bmatrix}^{(1)}$$

$$\Rightarrow \quad \begin{bmatrix} R\epsilon_g \\ RU\epsilon_g \\ E\epsilon_g \\ \epsilon_s \\ U\epsilon_s \\ P_s \end{bmatrix}_i^{n+1} = \begin{bmatrix} R\epsilon_g \\ RU\epsilon_g \\ E\epsilon_g \\ \epsilon_s \\ U\epsilon_s \\ P_s \end{bmatrix}_i^{n} - \frac{s}{2}\begin{bmatrix} RU\Delta^F\epsilon_g \\ RU^2\Delta^F\epsilon_g \\ UE\Delta^F\epsilon_g \\ U\Delta^F\epsilon_s \\ U^2\Delta^F\epsilon_s \\ 0 \end{bmatrix} - \frac{s}{2}\begin{bmatrix} RU\Delta^B\epsilon_g \\ RU^2\Delta^B\epsilon_g \\ UE\Delta^B\epsilon_g \\ U\Delta^B\epsilon_s \\ U^2\Delta^B\epsilon_s \\ 0 \end{bmatrix}^{n} + \frac{s^2}{2}\begin{bmatrix} RU^2\Delta^2\epsilon_g \\ RU^3\Delta^2\epsilon_g \\ U^2E\Delta^2\epsilon_g \\ U^2\Delta^2\epsilon_s \\ U^3\Delta^2\epsilon_s \\ 0 \end{bmatrix}^{n}$$

Thus,

$$\begin{bmatrix} \epsilon_g \\ \epsilon_g \\ \epsilon_g \\ \epsilon_s \\ \epsilon_s \\ P_s \end{bmatrix}_i^{n+1} = \begin{bmatrix} \epsilon_g \\ \epsilon_g \\ \epsilon_g \\ \epsilon_s \\ \epsilon_s \\ P_s \end{bmatrix}_i^{n} - \frac{s}{2}U\begin{bmatrix} \Delta^C\epsilon_g \\ \Delta^C\epsilon_g \\ \Delta^C\epsilon_g \\ \Delta^C\epsilon_s \\ \Delta^C\epsilon_s \\ 0 \end{bmatrix} + \frac{s^2}{2}U^2\begin{bmatrix} \Delta^2\epsilon_g \\ \Delta^2\epsilon_g \\ \Delta^2\epsilon_g \\ \Delta^2\epsilon_s \\ \Delta^2\epsilon_s \\ 0 \end{bmatrix}^{n}.$$

Hence, the MacCormack approach preserves the constants whilst advecting the volume fraction and granular temperature.

5.3 High Resolution Scheme

Hubbard & Garcia-Navarro [5] discussed an adapted form of Roe's scheme [13], which is a high resolution scheme. The scheme consists of

$$\mathbf{w}_i^{n+1} = \mathbf{w}_i^n - s(\mathbf{F}^*_{i+\frac{1}{2}} - \mathbf{F}^*_{i-\frac{1}{2}}) + s\mathbf{R}_i^* + \Delta t\mathbf{S}_i^n, \tag{5.1}$$

Roe Averages		
$\tilde{u}_g = \frac{\sqrt{(\epsilon_g\rho_g)_L}(u_g)_L + \sqrt{(\epsilon_g\rho_g)_R}(u_g)_R}{\sqrt{(\epsilon_g\rho_g)_L} + \sqrt{(\epsilon_g\rho_g)_R}}$	$\tilde{\epsilon}_g = \sqrt{(\epsilon_g)_R(\epsilon_g)_L}$	$\tilde{c}_g = \sqrt{(\gamma_g - 1)(\tilde{H}_g - \frac{1}{2}\tilde{u}_g^2)}$
$\tilde{H}_g = \frac{\sqrt{(\epsilon_g\rho_g)_L}(H_g)_L + \sqrt{(\epsilon_g\rho_g)_R}(H_g)_R}{\sqrt{(\epsilon_g\rho_g)_L} + \sqrt{(\epsilon_g\rho_g)_R}}$	$\tilde{p}_g = \frac{\tilde{\rho}_g}{\gamma_g}(\gamma_g - 1)(\tilde{H}_g - \frac{1}{2}\tilde{u}_g^2)$	$\tilde{\rho}_g = \frac{\sqrt{(\epsilon_g)_L}(\rho_g)_L + \sqrt{(\epsilon_g)_R}(\rho_g)_R}{\sqrt{(\epsilon_g)_L} + \sqrt{(\epsilon_g)_R}}$
Eigenvalues		
$\tilde{\lambda}_1 = \tilde{u}_g - \tilde{c}_g$	$\tilde{\lambda}_2 = \tilde{u}_g$	$\tilde{\lambda}_3 = \tilde{u}_g + \tilde{c}_g$
Eigenvectors		
$\tilde{\mathbf{e}}_1 = \begin{bmatrix} 1 \\ \tilde{u}_g - \tilde{c}_g \\ \tilde{H}_g - \tilde{u}_g\tilde{c}_g \end{bmatrix}$	$\tilde{\mathbf{e}}_2 = \begin{bmatrix} 1 \\ \tilde{u}_g \\ \frac{1}{2}\tilde{u}_g^2 \end{bmatrix}$	$\tilde{\mathbf{e}}_3 = \begin{bmatrix} 1 \\ \tilde{u}_g + \tilde{c}_g \\ \tilde{H}_g + \tilde{u}_g\tilde{c}_g \end{bmatrix}$
Wave Strengths		
$\tilde{\alpha}_2 = \frac{(\gamma_g - 1)}{\tilde{c}_g^2}\left(\left(\tilde{H}_g - \tilde{u}_g^2\right)\Delta(\epsilon_g\rho_g) + \tilde{u}_g\Delta(\epsilon_g\rho_g u_g) - \Delta(\epsilon_g E_g)\right)$		
$\tilde{\alpha}_1 = \frac{1}{2\tilde{c}_g}\left((\tilde{u}_g + \tilde{c}_g)\,\Delta(\epsilon_g\rho_g) - \Delta(\epsilon_g\rho_g u_g) - \tilde{c}_g\tilde{\alpha}_2\right)$		$\tilde{\alpha}_3 = \Delta(\epsilon_g\rho_g) - (\tilde{\alpha}_1 + \tilde{\alpha}_2)$
Inhomogeneous Terms		
$\tilde{\beta}_1 = \frac{\tilde{p}_g\left(2\tilde{c}_g\Delta(\epsilon_s u_s) - (\tilde{u}_g^2 - 2(\tilde{H}_g + \tilde{u}_g\tilde{c}_g))\Delta\epsilon_g\right)}{2\tilde{c}_g(\tilde{u}_g^2 - 2\tilde{H}_g)}$		$\tilde{\beta}_2 = \frac{-2\tilde{p}_g(\Delta(\epsilon_s u_s) + \tilde{u}_g\Delta\epsilon_g)}{\tilde{u}_g^2 - 2\tilde{H}_g}$
$\tilde{\beta}_3 = \frac{\tilde{p}_g\left(2\tilde{c}_g\Delta(\epsilon_s u_s) + (\tilde{u}_g^2 - 2(\tilde{H}_g - \tilde{u}_g\tilde{c}_g))\Delta\epsilon_g\right)}{2\tilde{c}_g(\tilde{u}_g^2 - 2\tilde{H}_g)}$		

Table 1: Roe Average Values for the Gas Phase

Roe Averages		
$\tilde{T}_s = \frac{\sqrt{(\epsilon_s)_L}(T_s)_L + \sqrt{(\epsilon_s)_R}(T_s)_R}{\sqrt{(\epsilon_s)_L} + \sqrt{(\epsilon_s)_R}}$	$\tilde{\epsilon}_s = \sqrt{(\epsilon_s)_R(\epsilon_s)_L}$	$\tilde{u}_s = \frac{\sqrt{(\epsilon_s)_L}(u_s)_L + \sqrt{(\epsilon_s)_R}(u_s)_R}{\sqrt{(\epsilon_s)_L} + \sqrt{(\epsilon_s)_R}}$
Eigenvalues		
$\tilde{\lambda}^S_{1,3} = \tilde{u}_s \mp \sqrt{\tilde{T}_s}$	$\tilde{\lambda}_2 = \tilde{u}_s$	$\tilde{\lambda}^P_{1,3} = \frac{4}{3}\tilde{u}_s + \frac{1}{3}\sqrt{\tilde{u}_s^2 + 15\tilde{T}_s}$
Eigenvectors		
$\tilde{\mathbf{e}}_k = \begin{bmatrix} 1 \\ \tilde{\lambda}_k \\ (\tilde{u}_s - \tilde{\lambda}_k)^2 \end{bmatrix}$		
Wave Strengths		
$\tilde{\alpha}_k = \frac{(\tilde{\lambda}_a\tilde{\lambda}_b - \tilde{u}_s^2)\Delta\epsilon_s + (2\tilde{u}_s - \tilde{\lambda}_a - \tilde{\lambda}_b)\Delta(\epsilon_s u_s) + \Delta(\epsilon_s T_s)}{(\tilde{\lambda}_k - \tilde{\lambda}_a)(\tilde{\lambda}_k - \tilde{\lambda}_b)}$ where $a \neq k \neq b$		
Inhomogeneous Terms		
$\tilde{\beta}_k = \frac{(2\tilde{u}_s - \tilde{\lambda}_a - \tilde{\lambda}_b)\tilde{r}_2 + \tilde{r}_3}{(\tilde{\lambda}_k - \tilde{\lambda}_a)(\tilde{\lambda}_k - \tilde{\lambda}_b)}$ where $a \neq k \neq b$		
$\tilde{r}_2 = -\frac{\tilde{\epsilon}_s}{\rho_s}\Delta p_g$	$\tilde{r}^S_3 = -\frac{2}{3}\tilde{\epsilon}_s\tilde{T}_s\Delta u_s$	$\tilde{r}^P_3 = \frac{2}{3}u_s\Delta(\epsilon_s T_s)$

Table 2: Roe Average Values for the Solids Phase (superscripts denote formulation)

with numerical flux-function

$$\mathbf{F}^*_{i+\frac{1}{2}} = \frac{1}{2}(\mathbf{F}^n_{i+1} + \mathbf{F}^n_i) - \frac{1}{2}\sum_{k=1}^{6}\left[\tilde{\alpha}_k|\tilde{\lambda}_k|(1-\Phi(\tilde{\theta}_k)(1-|\tilde{\nu}_k|))\tilde{\mathbf{e}}_k\right]_{i+\frac{1}{2}}.$$

The inhomogeneous terms not containing first order derivatives, $\mathbf{S}$, are approximated using a pointwise approach,

$$\mathbf{S}^n_i = \begin{bmatrix} 0 \\ -\beta(u_g - u_s) \\ -\beta u_g(u_g - u_s) \\ 0 \\ \frac{\beta}{\rho_s}(u_g - u_s) \\ -\frac{2}{\rho_s}\beta T_s \end{bmatrix}^n_i$$

and the inhomogeneous terms containing first order derivatives, $\mathbf{R}$, are approximated by using an upwind approach,

$$\mathbf{R}^*_i = \mathbf{R}^-_{i+\frac{1}{2}} + \mathbf{R}^+_{i-\frac{1}{2}}, \tag{5.2}$$

where

$$\mathbf{R}^\pm_{i+\frac{1}{2}} = \frac{1}{2}\sum_{k=1}^{6}\left[\tilde{\beta}_k\tilde{\mathbf{e}}_k(1 \pm \mathrm{sgn}(\tilde{\lambda}_k)(1-\Phi(\tilde{\theta}_k)(1-|\tilde{\nu}_k|)))\right]_{i+\frac{1}{2}}.$$

The step sizes in space and time are Δx and Δt with i and n denoting the spatial and time grid number, respectively. The upstream and downstream boundaries are at x_0 and x_I (I is the total number of spatial grid points), t_N is the final time,

$$s = \frac{\Delta t}{\Delta x}, \quad \tilde{\nu}_k = s\tilde{\lambda}_k, \quad \tilde{\theta}_k = \frac{(\tilde{\alpha}_k)_{J+\frac{1}{2}}}{(\tilde{\alpha}_k)_{J+\frac{1}{2}}}, \quad J = i - \mathrm{sgn}(\tilde{\nu}_k)_{i+\frac{1}{2}},$$

and the minmod flux-limiter [15],

$$\Phi(\theta) = \max(0, \min(1, \theta)),$$

is used.

Here, the $\tilde{}$ is called the Roe average and $\tilde{\lambda}$, $\tilde{\mathbf{e}}$ and $\tilde{\alpha}$ are the eigenvalues, eigenvectors and wave strengths of the Roe averaged Jacobian matrix, $\tilde{\mathbf{A}}$. The Roe averaged eigenvalues, eigenvectors, wave strengths and inhomogeneous terms are determined from the Roe decomposition (see [13, 5, 6] for more details)

$$\Delta\mathbf{F} = \sum_{k=1}^{p}\tilde{\alpha}_k\tilde{\lambda}_k\tilde{\mathbf{e}}_k = \tilde{\mathbf{A}}\Delta\mathbf{w} \quad \text{and} \quad \tilde{\mathbf{R}} = \frac{1}{\Delta x}\sum_{k=1}^{p}\tilde{\beta}_k\tilde{\mathbf{e}}_k,$$

where $\Delta\mathbf{w} = \mathbf{w}_R - \mathbf{w}_L$ and p is the number of components in the system. A summary of the Roe averages is given in Tables 1 & 2 for the gas and solid phase, respectively.

5.3.1 Accuracy for Advection Test Case: Gas Phase

We now analyse the first order version of the scheme, i.e. $\Phi = 0$. We first simplify the Roe averages for the test case. Using,

$$\rho_g H_g = E_g + p_g, \quad c_g^2 = \frac{p_g \gamma_g}{\rho_g},$$

we obtain

$$\begin{aligned}
\tilde{\alpha}_2 &= \frac{(\gamma_g - 1)}{\tilde{c}_g^2} \left(\left(\tilde{H}_g - \tilde{u}_g^2 \right) \Delta(\epsilon_g \rho_g) + \tilde{u}_g \Delta(\epsilon_g \rho_g u_g) - \Delta(\epsilon_g E_g) \right) \\
&= \frac{(\gamma_g - 1)}{\tilde{c}_g^2} \left(\left(H - U^2 \right) R \Delta\epsilon_g + R U^2 \Delta\epsilon_g - E \Delta\epsilon_g \right) \\
&= \frac{(\gamma_g - 1)}{\tilde{c}_g^2} \left(RH - E \right) \Delta\epsilon_g \\
&= \frac{P_g(\gamma_g - 1)}{\tilde{c}_g^2} \Delta\epsilon_g = \frac{R}{\gamma_g}(\gamma_g - 1)\Delta\epsilon_g,
\end{aligned}$$

$$\begin{aligned}
\tilde{\alpha}_1 &= \frac{1}{2\tilde{c}_g} \left((\tilde{u}_g + \tilde{c}_g) \Delta(\epsilon_g \rho_g) - \Delta(\epsilon_g \rho_g u_g) - \tilde{c}_g \tilde{\alpha}_2 \right) \\
&= \frac{1}{2\tilde{c}_g} \left((U + \tilde{c}_g) R \Delta\epsilon_g - R U \Delta\epsilon_g - \tilde{c}_g \frac{R}{\gamma_g}(\gamma_g - 1)\Delta\epsilon_g \right) \\
&= \frac{1}{2\tilde{c}_g} \left(\tilde{c}_g R - \tilde{c}_g \frac{R}{\gamma_g}(\gamma_g - 1) \right) \Delta\epsilon_g \\
&= \frac{R}{2\gamma_g} \left(\gamma_g - (\gamma_g - 1) \right) \Delta\epsilon_g = \frac{R}{2\gamma_g} \Delta\epsilon_g,
\end{aligned}$$

and

$$\begin{aligned}
\tilde{\alpha}_3 &= \Delta(\epsilon_g \rho_g) - (\tilde{\alpha}_1 + \tilde{\alpha}_2) \\
&= R\Delta\epsilon_g - (\frac{R}{2\gamma_g}\Delta\epsilon_g + \frac{R}{\gamma_g}(\gamma_g - 1)\Delta\epsilon_g) \\
&= \frac{R}{2\gamma_g} \left(2\gamma_g - 1 - 2(\gamma_g - 1) \right) \Delta\epsilon_g = \frac{R}{2\gamma_g} \Delta\epsilon_g.
\end{aligned}$$

Also,

$$\begin{aligned}
\tilde{\beta}_1 &= \frac{\tilde{p}_g\left(2\tilde{c}_g\Delta(\epsilon_s u_s) - (\tilde{u}_g^2 - 2(\tilde{H}_g + \tilde{u}_g\tilde{c}_g))\Delta\epsilon_g\right)}{2\tilde{c}_g(\tilde{u}_g^2 - 2\tilde{H}_g)} \\
&= \frac{P_g\left(2\tilde{c}_g U\Delta\epsilon_s + (U^2 - 2(H + U\tilde{c}_g))\Delta\epsilon_s\right)}{2\tilde{c}_g(U^2 - 2H)} \\
&= \frac{P_g(U^2 - 2H)\Delta\epsilon_s}{2\tilde{c}_g(U^2 - 2H)} = \frac{P_g\Delta\epsilon_s}{2\tilde{c}_g} = -\frac{R\tilde{c}_g}{2\gamma_g}\Delta\epsilon_g,
\end{aligned}$$

$$\tilde{\beta}_2 = \frac{-2\tilde{p}_g(\Delta(\epsilon_s u_s) + \tilde{u}_g\Delta\epsilon_g)}{\tilde{u}_g^2 - 2\tilde{H}_g} = \frac{-2P_g(U\Delta\epsilon_s - U\Delta\epsilon_s)}{U^2 - 2H} = 0$$

and

$$\begin{aligned}
\tilde{\beta}_3 &= \frac{\tilde{p}_g\left(2\tilde{c}_g\Delta(\epsilon_s u_s) + (\tilde{u}_g^2 - 2(\tilde{H}_g - \tilde{u}_g\tilde{c}_g))\Delta\epsilon_g\right)}{2\tilde{c}_g(\tilde{u}_g^2 - 2\tilde{H}_g)} \\
&= \frac{P_g\left(-2\tilde{c}_g U + (U^2 - 2(H - U\tilde{c}_g))\right)\Delta\epsilon_g}{2\tilde{c}_g(U^2 - 2H)} \\
&= \frac{P_g(U^2 - 2H)\Delta\epsilon_g}{2\tilde{c}_g(U^2 - 2H)} = \frac{P_g}{2\tilde{c}_g}\Delta\epsilon_g = \frac{R\tilde{c}_g}{2\gamma_g}\Delta\epsilon_g.
\end{aligned}$$

Thus,

$$\begin{aligned}
\mathbf{F}^*_{i\pm\frac{1}{2}} &= \frac{1}{2}\begin{bmatrix} RU \\ RU^2 + P_g \\ U(E + P_g) \end{bmatrix}((\epsilon_g)_R + (\epsilon_g)_L) \\
&-\frac{1}{2}\left(\begin{bmatrix} 1 \\ U - c_g \\ H - Uc_g \end{bmatrix}|U - c_g|\frac{R}{2\gamma_g} + \begin{bmatrix} 1 \\ U \\ \frac{1}{2}U^2 \end{bmatrix}|U|\frac{R}{\gamma_g}(\gamma - 1) + \begin{bmatrix} 1 \\ U + c_g \\ H + Uc_g \end{bmatrix}|U + c_g|\frac{R}{2\gamma_g}\right)\Delta\epsilon_g
\end{aligned}$$

$$\begin{aligned}
\Rightarrow \quad \mathbf{F}^*_{i\pm\frac{1}{2}} &= \frac{1}{2}\begin{bmatrix} RU \\ RU^2 + P_g \\ U(E + P_g) \end{bmatrix}((\epsilon_g)_R + (\epsilon_g)_L) \\
&- \frac{R}{2\gamma_g}\begin{bmatrix} \frac{1}{2}|U - c_g| + |U|(\gamma_g - 1) + \frac{1}{2}|U + c_g| \\ \frac{1}{2}|U - c_g|(U - c_g) + |U|U(\gamma_g - 1) + \frac{1}{2}|U + c_g|(U + c_g) \\ \frac{1}{2}|U - c_g|(H - Uc_g) + \frac{1}{2}U^2|U|(\gamma_g - 1) + \frac{1}{2}|U + c_g|(H + Uc_g) \end{bmatrix}\Delta\epsilon_g
\end{aligned}$$

We now consider only a positive velocity, i.e. $U > 0$. For subcritical flow,

$$c_g > U > 0 \quad \Rightarrow \quad |U - c_g| = c_g - U, \quad |U| = U \quad \text{and} \quad |U + c_g| = U + c_g,$$

thus

$$\mathbf{F}^*_{i\pm\frac{1}{2}} = \frac{1}{2}\begin{bmatrix} RU \\ RU^2 + P_g \\ U(E+P_g) \end{bmatrix}((\epsilon_g)_R + (\epsilon_g)_L)$$
$$- \frac{R}{2\gamma_g}\begin{bmatrix} \frac{1}{2}(-U+c_g) + U(\gamma_g - 1) + \frac{1}{2}(U+c_g) \\ \frac{1}{2}(-U+c_g)(U-c_g) + U^2(\gamma_g-1) + \frac{1}{2}(U+c_g)(U+c_g) \\ \frac{1}{2}(-U+c_g)(H-Uc_g) + \frac{1}{2}U^3(\gamma_g-1) + \frac{1}{2}(U+c_g)(H+Uc_g) \end{bmatrix}\Delta\epsilon_g$$

$$\Rightarrow \quad \mathbf{F}^*_{i\pm\frac{1}{2}} = \frac{1}{2}\begin{bmatrix} RU \\ RU^2 + P_g \\ U(E+P_g) \end{bmatrix}((\epsilon_g)_R + (\epsilon_g)_L) - \frac{R}{2\gamma_g}\begin{bmatrix} c_g + U(\gamma_g-1) \\ 2Uc_g + U^2(\gamma_g-1) \\ (H+U^2)c_g + \frac{1}{2}U^3(\gamma_g-1) \end{bmatrix}\Delta\epsilon_g.$$

The source term approximation becomes

$$\mathbf{R}^{\pm}_{i+\frac{1}{2}} = \frac{1}{2}\left(\begin{bmatrix} 1 \\ U-c_g \\ H-Uc_g \end{bmatrix}\left(-\frac{Rc_g}{2\gamma_g}\right)(1\pm(-1)) + \begin{bmatrix} 1 \\ U+c_g \\ H+Uc_g \end{bmatrix}\left(\frac{Rc_g}{2\gamma_g}\right)(1\pm(1))\right)\Delta\epsilon_g$$

$$\Rightarrow \quad \mathbf{R}^{\pm}_{i+\frac{1}{2}} = \begin{bmatrix} \pm 1 \\ c_g \pm U \\ Uc_g \pm H \end{bmatrix}\frac{Rc_g}{2\gamma_g}\Delta\epsilon_g.$$

Now,

$$-\mathbf{F}^*_{i+\frac{1}{2}} + \mathbf{R}^-_{i+\frac{1}{2}} = -\frac{1}{2}\begin{bmatrix} RU \\ RU^2 + P_g \\ U(E+P_g) \end{bmatrix}((\epsilon_g)_{i+1} + (\epsilon_g)_i) + \frac{R}{2\gamma_g}\begin{bmatrix} c_g + U(\gamma_g-1) \\ 2Uc_g + U^2(\gamma_g-1) \\ (H+U^2)c_g + \frac{1}{2}U^3(\gamma_g-1) \end{bmatrix}\Delta\epsilon_g$$
$$+ \begin{bmatrix} -1 \\ c_g - U \\ Uc_g - H \end{bmatrix}\frac{Rc_g}{2\gamma_g}\Delta\epsilon_g$$

$$\Rightarrow \quad -\mathbf{F}^*_{i+\frac{1}{2}} + \mathbf{R}^-_{i+\frac{1}{2}} = -\frac{1}{2}\begin{bmatrix} RU \\ RU^2 + P_g \\ U(E+P_g) \end{bmatrix}((\epsilon_g)_{i+1} + (\epsilon_g)_i)$$
$$+ \frac{R}{2\gamma_g}\begin{bmatrix} c_g + U(\gamma_g-1) - c_g \\ 2Uc_g + U^2(\gamma_g-1) - Uc_g + c_g^2 \\ (H+U^2)c_g + \frac{1}{2}U^3(\gamma_g-1) + Uc_g^2 - Hc_g \end{bmatrix}\Delta\epsilon_g$$

$$\Rightarrow \quad -\mathbf{F}^*_{i+\frac{1}{2}} + \mathbf{R}^-_{i+\frac{1}{2}} = -\frac{1}{2}\begin{bmatrix} RU \\ RU^2 + P_g \\ U(E+P_g) \end{bmatrix}((\epsilon_g)_{i+1} + (\epsilon_g)_i)$$
$$+ \frac{R}{2\gamma_g}\begin{bmatrix} U(\gamma_g - 1) \\ Uc_g + U^2(\gamma_g - 1) + c_g^2 \\ U^2 c_g + \frac{1}{2}U^3(\gamma_g - 1) + Uc_g^2 \end{bmatrix}\Delta\epsilon_g.$$

Here, we can see that the scheme will produce inaccurate results since the flux-function and source terms do not balance. However, the scheme is exact when $U = 0$. For supercritical flow,

$$U > c_g > 0 \quad \Rightarrow \quad |U - c_g| = U - c_g, \quad |U| = U \quad \text{and} \quad |U + c_g| = U + c_g,$$

thus

$$\mathbf{F}^*_{i\pm\frac{1}{2}} = \frac{1}{2}\begin{bmatrix} RU \\ RU^2 + P_g \\ U(E+P_g) \end{bmatrix}((\epsilon_g)_R + (\epsilon_g)_L)$$
$$- \frac{R}{2\gamma_g}\begin{bmatrix} \frac{1}{2}(U - c_g) + U(\gamma_g - 1) + \frac{1}{2}(U + c_g) \\ \frac{1}{2}(U - c_g)(U - c_g) + U^2(\gamma_g - 1) + \frac{1}{2}(U + c_g)(U + c_g) \\ \frac{1}{2}(U - c_g)(H - Uc_g) + \frac{1}{2}U^3(\gamma_g - 1) + \frac{1}{2}(U + c_g)(H + Uc_g) \end{bmatrix}\Delta\epsilon_g$$

$$\Rightarrow \quad \mathbf{F}^*_{i\pm\frac{1}{2}} = \frac{1}{2}\begin{bmatrix} RU \\ RU^2 + P_g \\ U(E+P_g) \end{bmatrix}((\epsilon_g)_R + (\epsilon_g)_L) - \frac{R}{2\gamma_g}\begin{bmatrix} U\gamma_g \\ c_g^2 + U^2\gamma_g \\ UH + Uc_g^2 + \frac{1}{2}U^3(\gamma_g - 1) \end{bmatrix}\Delta\epsilon_g$$

and since

$$H = \frac{\gamma_g E}{R} - \frac{1}{2}(\gamma_g - 1)U^2,$$

$$\Rightarrow \quad \mathbf{F}^*_{i\pm\frac{1}{2}} = \frac{1}{2}\begin{bmatrix} RU \\ RU^2 + P_g \\ U(E+P_g) \end{bmatrix}((\epsilon_g)_R + (\epsilon_g)_L) - \frac{R}{2\gamma_g}\begin{bmatrix} U\gamma_g \\ (\frac{P_g\gamma_g}{R}) + U^2\gamma_g \\ (\frac{UP_g\gamma_g}{R}) + (\frac{UE\gamma_g}{R}) \end{bmatrix}\Delta\epsilon_g$$

$$\Rightarrow \quad \mathbf{F}^*_{i\pm\frac{1}{2}} = \frac{1}{2}\begin{bmatrix} RU \\ RU^2 + P_g \\ U(E+P_g) \end{bmatrix}((\epsilon_g)_R + (\epsilon_g)_L) - \frac{1}{2}\begin{bmatrix} RU \\ RU^2 + P_g \\ U(E+P_g) \end{bmatrix}\Delta\epsilon_g.$$

Therefore,

$$\mathbf{F}^*_{i\pm\frac{1}{2}} = \begin{bmatrix} RU \\ RU^2 + P_g \\ U(E+P_g) \end{bmatrix}(\epsilon_g)_L.$$

The source term approximation becomes

$$\mathbf{R}^{\pm}_{i+\frac{1}{2}} = \frac{1}{2}\left(\begin{bmatrix} 1 \\ U - c_g \\ H - Uc_g \end{bmatrix}\left(-\frac{Rc_g}{2\gamma_g}\right)(1 \pm (1)) + \begin{bmatrix} 1 \\ U + c_g \\ H + Uc_g \end{bmatrix}\left(\frac{Rc_g}{2\gamma_g}\right)(1 \pm (1))\right)\Delta\epsilon_g$$

$$\Rightarrow \quad \mathbf{R}^{-}_{i+\frac{1}{2}} = 0 \quad \text{and} \quad \mathbf{R}^{+}_{i+\frac{1}{2}} = \begin{bmatrix} 0 \\ c_g \\ Uc_g \end{bmatrix}\frac{Rc_g}{\gamma_g}\Delta\epsilon_g.$$

Now,

$$-\mathbf{F}^{*}_{i+\frac{1}{2}} + \mathbf{R}^{-}_{i+\frac{1}{2}} = -\begin{bmatrix} RU \\ RU^2 + P_g \\ U(E + P_g) \end{bmatrix}(\epsilon_g)_i$$

and

$$\mathbf{F}^{*}_{i-\frac{1}{2}} + \mathbf{R}^{+}_{i-\frac{1}{2}} = \begin{bmatrix} RU \\ RU^2 + P_g \\ U(E + P_g) \end{bmatrix}(\epsilon_g)_{i-1} + \begin{bmatrix} 0 \\ c_g \\ Uc_g \end{bmatrix}\frac{Rc_g}{\gamma_g}\Delta\epsilon_g$$

$$\Rightarrow \quad \mathbf{F}^{*}_{i-\frac{1}{2}} + \mathbf{R}^{+}_{i-\frac{1}{2}} = \begin{bmatrix} RU \\ RU^2 + P_g \\ U(E + P_g) \end{bmatrix}(\epsilon_g)_{i-1} + \begin{bmatrix} 0 \\ P_g \\ UP_g \end{bmatrix}\Delta\epsilon_g$$

$$\Rightarrow \quad \mathbf{F}^{*}_{i-\frac{1}{2}} + \mathbf{R}^{+}_{i-\frac{1}{2}} = \begin{bmatrix} 0 \\ P_g \\ UP_g \end{bmatrix}(\epsilon_g)_i + \begin{bmatrix} RU \\ RU^2 \\ UE \end{bmatrix}(\epsilon_g)_{i-1}.$$

Hence,

$$\begin{bmatrix} R\epsilon_g \\ RU\epsilon_g \\ E\epsilon_g \end{bmatrix}_i^{n+1} = \begin{bmatrix} R\epsilon_g \\ RU\epsilon_g \\ E\epsilon_g \end{bmatrix}_i^{n} - s\left(\begin{bmatrix} RU \\ RU^2 + P_g \\ U(E + P_g) \end{bmatrix}(\epsilon_g)_i - \begin{bmatrix} 0 \\ P_g \\ UP_g \end{bmatrix}(\epsilon_g)_i - \begin{bmatrix} RU \\ RU^2 \\ UE \end{bmatrix}(\epsilon_g)_{i-1}\right)$$

$$\Rightarrow \quad \begin{bmatrix} R\epsilon_g \\ RU\epsilon_g \\ E\epsilon_g \end{bmatrix}_i^{n+1} = \begin{bmatrix} R\epsilon_g \\ RU\epsilon_g \\ E\epsilon_g \end{bmatrix}_i^{n} - s\begin{bmatrix} RU \\ RU^2 \\ UE \end{bmatrix}\Delta^B\epsilon_g.$$

Here, we can see that the scheme preserves the values of the constants and advects the volume fraction.

5.3.2 Accuracy for Advection Test Case: Solids Phase

We continue to analyse the first order version of the scheme, i.e. $\Phi = 0$, with Formulation AES for the solids phase. We first simplify the Roe averages for the test case. Here,

$$\tilde{\alpha}_{1,3} = 0, \quad \tilde{\alpha}_2 = \Delta\epsilon_s \quad \text{and} \quad \tilde{\beta}_k = 0.$$

Thus,

$$\mathbf{F}^*_{i\pm\frac{1}{2}} = \frac{1}{2}\begin{bmatrix} U((\epsilon_s)_R + (\epsilon_s)_L) \\ U^2((\epsilon_s)_R + (\epsilon_s)_L) + 2P_s \\ U((\epsilon_s T_s)_R + (\epsilon_s T_s)_L) \end{bmatrix} - \frac{1}{2}\begin{bmatrix} 1 \\ U \\ 0 \end{bmatrix} |U|\Delta\epsilon_s$$

and by assuming

$$U > 0 \quad \Rightarrow \quad |U| = U,$$

$$\mathbf{F}^*_{i\pm\frac{1}{2}} = \frac{1}{2}\begin{bmatrix} U((\epsilon_s)_R + (\epsilon_s)_L) - U\Delta\epsilon_s \\ U^2((\epsilon_s)_R + (\epsilon_s)_L) + 2P_s - U^2\Delta\epsilon_s \\ 2UP_s \end{bmatrix}$$

$$\Rightarrow \quad \mathbf{F}^*_{i\pm\frac{1}{2}} = \begin{bmatrix} U(\epsilon_s)_L \\ U^2(\epsilon_s)_L + P_s \\ UP_s \end{bmatrix}$$

Hence,

$$\begin{bmatrix} \epsilon_s \\ U\epsilon_s \\ P_s \end{bmatrix}_i^{n+1} = \begin{bmatrix} \epsilon_s \\ U\epsilon_s \\ P_s \end{bmatrix}_i^{n} - s\left(\begin{bmatrix} U(\epsilon_s)_i \\ U^2(\epsilon_s)_i + P_s \\ UP_s \end{bmatrix} - \begin{bmatrix} U(\epsilon_s)_{i-1} \\ U^2(\epsilon_s)_{i-1} + P_s \\ UP_s \end{bmatrix}\right)$$

$$\Rightarrow \quad \begin{bmatrix} \epsilon_s \\ U\epsilon_s \\ P_s \end{bmatrix}_i^{n+1} = \begin{bmatrix} \epsilon_s \\ U\epsilon_s \\ P_s \end{bmatrix}_i^{n} - s\begin{bmatrix} U \\ U^2 \\ 0 \end{bmatrix}\Delta^B\epsilon_s.$$

Here, we can see that the solids phase preserves all constants and correctly advects the solids volume fraction whist ensuring the solids pressure remains a constant. The same result can be shown for Formulation AEP.

6 Numerical Results

We now investigate the behaviour of the different models and schemes for the gas-solid flow as discussed in Section 2.2. In order to compare the different models, we consider a

variety of test cases. Unless stated otherwise, the domain is of length 100 m and schemes are used with $\Delta x = 1$ m (i.e. 100 grid points) and a Courant number $\nu = 0.8$.

We only solve the models when they are hyperbolic and require appropriate initial and boundary conditions for each test case. Unless otherwise stated, the numerical scheme uses free flow boundary conditions,

$$\mathbf{w}_{-i}^{n+1} = \mathbf{w}_0^n \quad \text{and} \quad \mathbf{w}_{I+i}^{n+1} = \mathbf{w}_I^n,$$

We now compare the results of the different schemes for a variety of different test cases : the analytical solution (AnS), the Lax-Wendroff Scheme (LxW), MacCormack's scheme (MaC), Roe's first order scheme (RFO) and the high resolutions scheme (RHR).

6.1 Advection Test Problem

For the first test case, we compare the accuracy of the different schemes when applied to the advection test case for which an analytical solution can be obtained. The analytical solution is derived by assuming that the gas density and both phase velocities are constants,

$$\rho_g(x,t) = R, \quad E_g(x,t) = E \quad \text{and} \quad u_g(x,t) = u_s(x,t) = U,$$

then the model simplifies to

$$(\epsilon_s)_t + U(\epsilon_s)_x = 0, \quad p_s(x,t) = P \quad \text{and} \quad (T_s)_t + U(T_s)_x = 0,$$

where P is a constant. Thus, we obtain the analytical solution

$$\epsilon_s(x,t) = \epsilon_s(x - Ut, 0) \quad \text{and} \quad T_s(x,t) = \frac{P}{\epsilon_s}.$$

To simulate a solids pulse propagating downstream, we use the initial conditions,

$$\epsilon_s(x,0) = \begin{cases} 0.1 + 0.1\sin^2\left(\frac{\pi}{10}(x-5)\right) & \text{if } 5 \le x \le 15 \\ 0.1 & \text{otherwise} \end{cases}$$

with

$$R = 1.2885, \quad E = 1000 \quad U = 5 \quad \text{and} \quad P = 0.01.$$

Figure 6.1, illustrates the results of the schemes at $t = 10$s for Formulation AES. A spatial step-size of $\Delta x = 0.1$ was used. Here, we can see that small numerical errors have occurred in all of the schemes with the exception of the MacCormack scheme. This is in agreement with the analytical analysis of the schemes we presented in the previous section. Although the numerical error is small, it could be enhanced for other test cases.

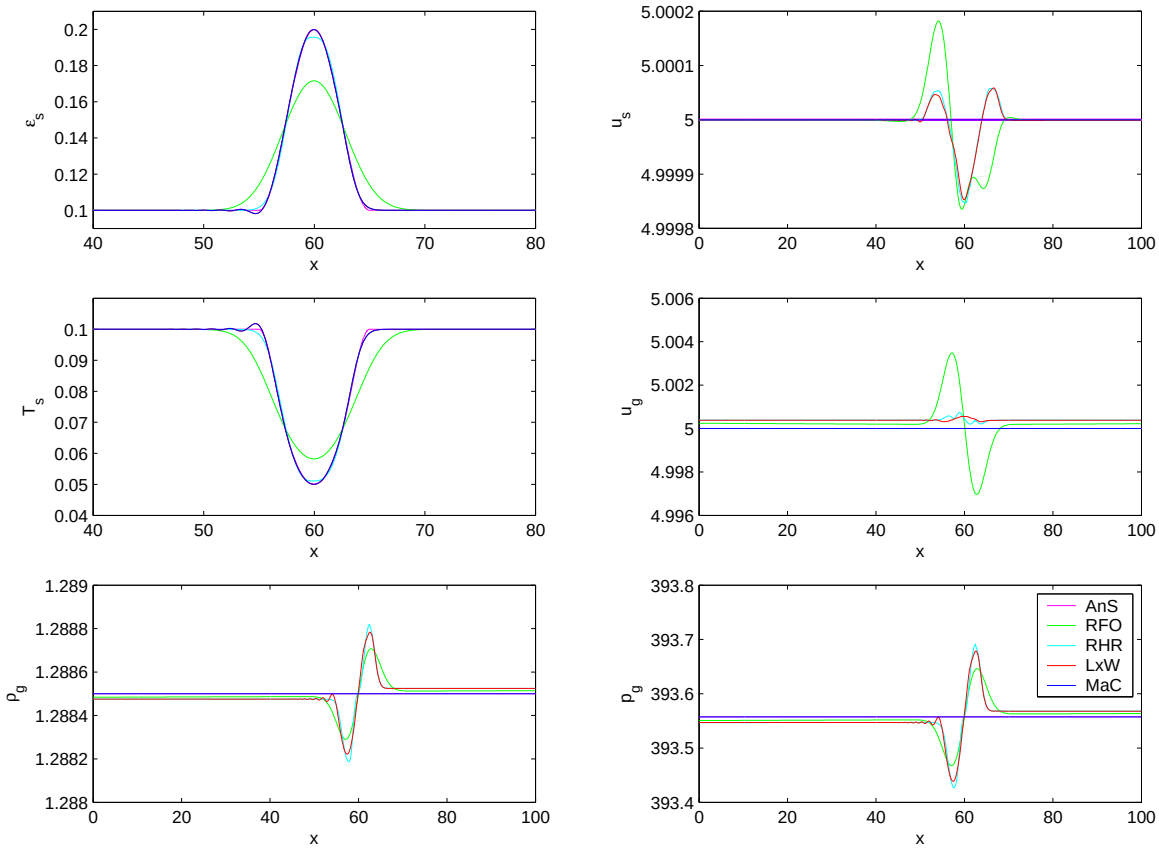

Figure 6.1: Results of the Advection Test Problem at $t = 10$ s (Formulation AES).

6.2 Gas Shock Tube Problem

In order to test the gas phase of Model A-EE, we use the Shock Tube problem of Sod [14] whose domain is 1m long and the initial conditions are

$$\epsilon_s(x,0) = 0, \quad u_s(x,0) = 0, \quad T_s(x,0) = 0,$$

$$\rho_g(x,0) = \begin{cases} 1 & \text{if } x < 0.5, \\ 0.125 & \text{if } x \geq 0.5, \end{cases} \quad p_g(x,0) = \begin{cases} 1 & \text{if } x < 0.5, \\ 0.1 & \text{if } x \geq 0.5, \end{cases} \quad \text{and} \quad u_g(x,0) = 0.$$

Figure 6.2, illustrates the results of the schemes at $t = 0.25$s for Formulation AES. A spatial step-size of $\Delta x = 0.001$ was used. The analytical solution (AnS) was obtained from the NUMERICA library [16]. Here, we can see that Roe's first order scheme and the high resolution scheme have produced results close to the analytical solution. All schemes preserved the constant values for the solids phase, but the Lax-Wendroff scheme

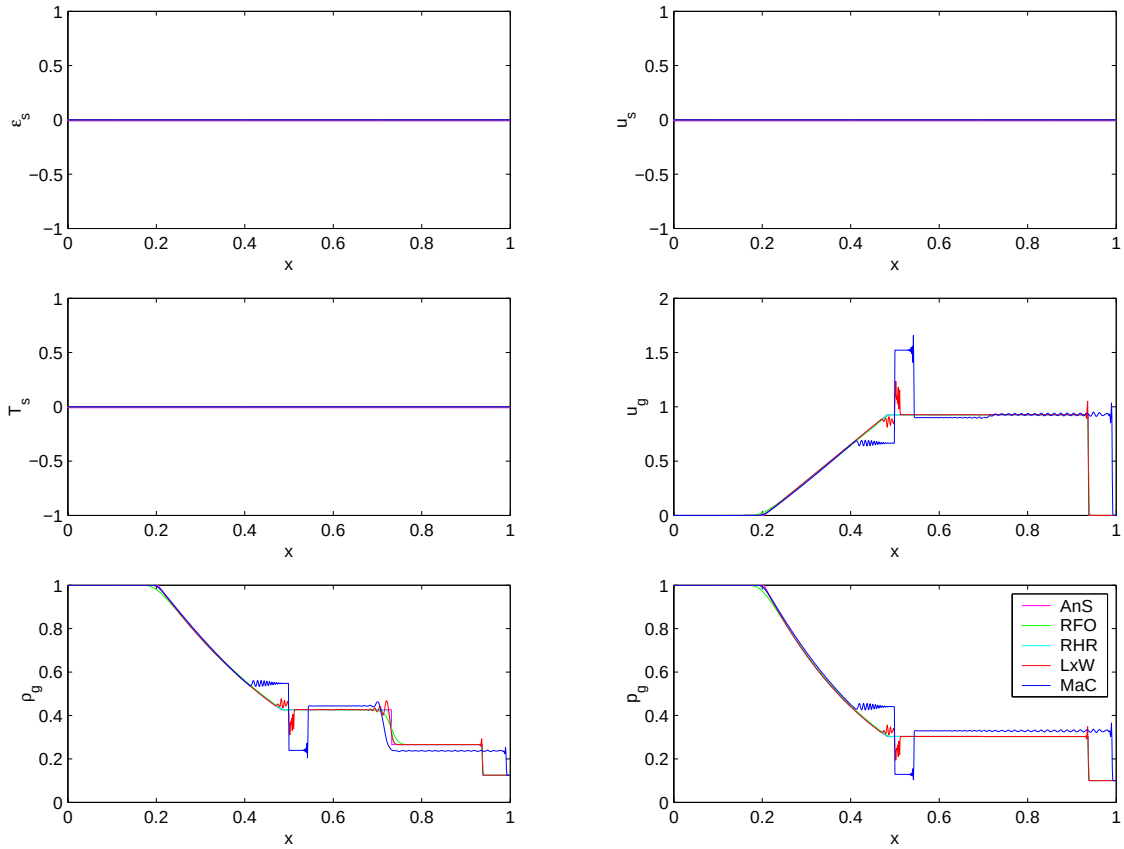

Figure 6.2: Results of the Advection Test Problem at $t = 10$ s (Formulation AES).

and MacCormack's scheme both produced spurious numerical oscillations. Moreover, the MacCormack approach did not accurately calculate the shock speed of the right shock.

6.3 Square Pulse Test Problem

For the third test case, we simulate a square pulse of solids in the centre of the domain, which is at rest. In this simple simulation, we imagine that "walls" at $x = 40$ m and $x = 60$ m confine the solids to the region $40 < x < 60$ of the domain and they are kept in suspension by a "stirrer". The "walls" are then removed at time $t = 0$ and the solids are allowed to move freely. The initial conditions for this test case consists of

$$\rho_g(x, 0) = 1.2885, \quad u_g(x, 0) = u_s(x, 0) = 0, \quad T_s(x, 0) = 0.1\epsilon_s(x, 0)$$

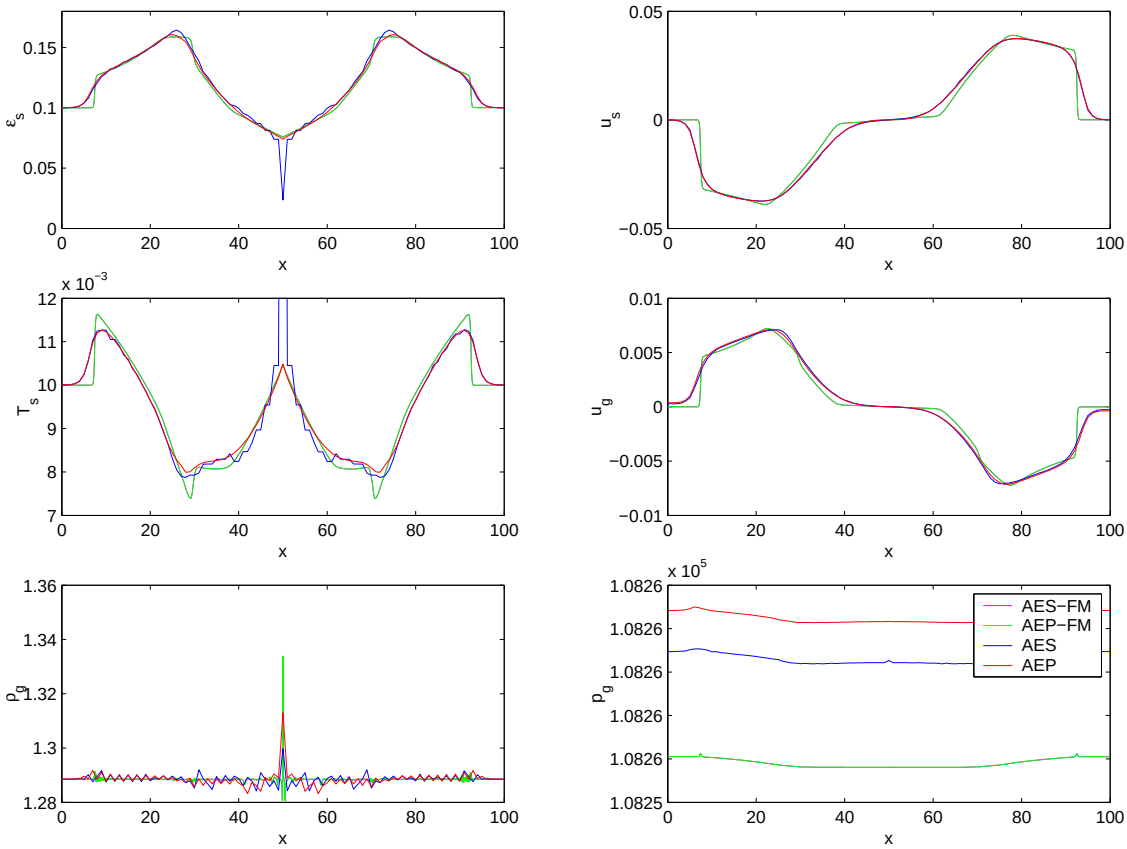

Figure 6.3: Results for the Square Pulse Test Problem at $t = 200$ s.

and

$$\epsilon_s(x,0) = \begin{cases} 0.2 & \text{if } 40 \le x \le 60, \\ 0.1 & \text{otherwise.} \end{cases}$$

For the isentropic model (Model A), the gas pressure was

$$p_g(\rho_g) = C_p \rho_g^{\gamma_g} \quad \text{where} \quad C_p = 75916.16.$$

It is desirable to obtain a corresponding value of the initial gas pressure for Model A-EE. Since the initial gas density is a constant, we let $p_g^* = 108256.1118$ and use this value in order to determine the initial total energy per unit volume

$$E_g(x,0) = \frac{p_g^*}{\gamma_g - 1} + \frac{1}{2}\rho_g(x,0)u_g(x,0)^2.$$

Figure 6.3 illustrates the results of both formulations using the high resolution scheme. The fine mesh results were calculated using $\Delta x = 0.1$. Here, we can see that the numerical

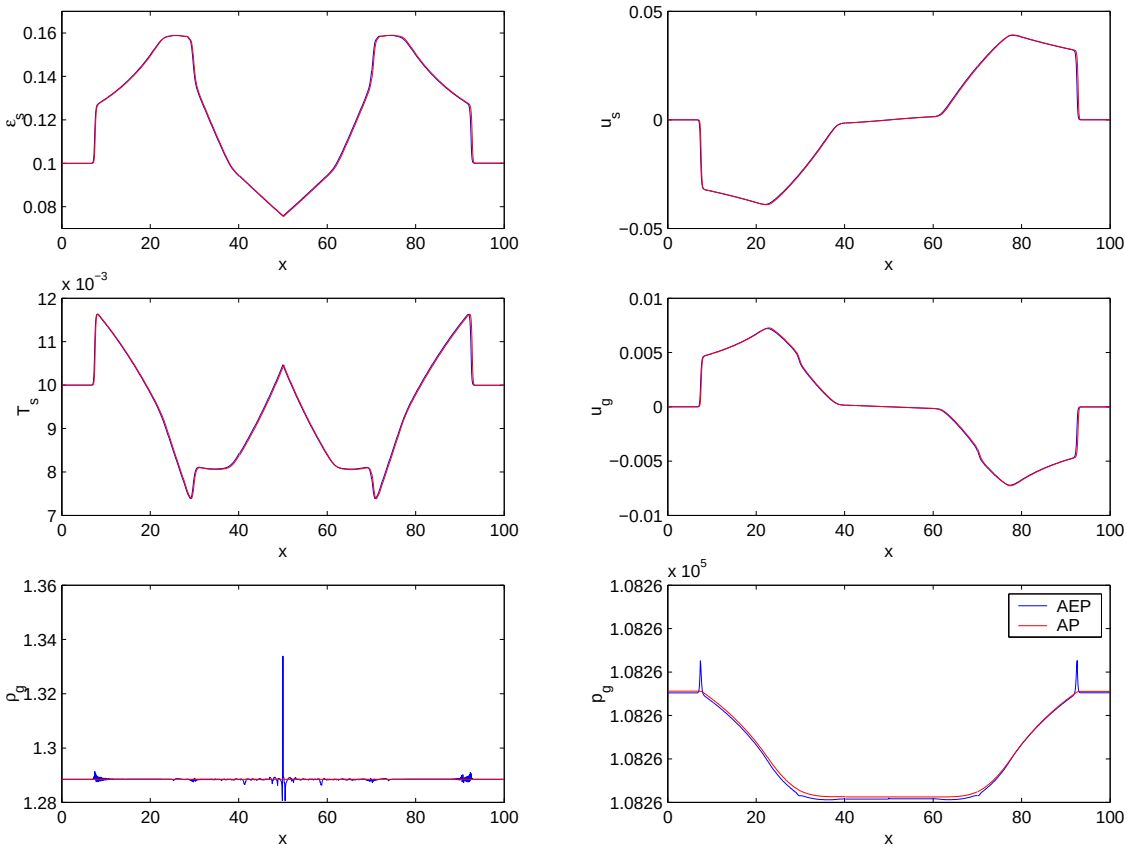

Figure 6.4: Comparison of the Isentropic (AP) and non-isentropic (AEP) results for the Square Pulse Test Problem at $t = 200$.

scheme produced spurious numerical oscillations in the gas density. Formulation AES produced the same numerical error at the stagnation point $x = 50$ as discussed in Hudson & Harris [7] whereas Formulation AEP did not produce this error. The error is caused by the approximation of $-p_s(u_s)_x$ in the fluctuating energy equation (2.6). Formulation AEP rectifies this problem by rewriting the problematic term by using the product rule.

Figure 6.4 compares the results of the isentropic model (Model AP), see Hudson & Harris [7] with the results of Model AEP. Here, we can see (with the exception of the numerical error in the gas density) that both models produced practically identical results. Thus, the assumption of an isentropic gas phase is valid for the regime of interest described in this paper. This is due to the gas density and pressure being almost constant (at most smooth with no discontinuities present in either of these two variables).

7 Conclusion

We have extended the isentropic Eulerian gas-solid two-phase model (as discussed by Hudson & Harris [7]) to include a gas energy equation and investigated two different formulations of this model. Three different schemes were used to discretise the model and a thorough analysis was performed to determine the robustness and accuracy of these schemes. As expected, the results of both second order schemes suffered from spurious numerical oscillations whereas the high resolution scheme minimised these oscillations. However, the high resolution scheme produced numerical errors in the results. Even though the high resolution scheme satisfies all the u-properties of Roe [13] and has been discretised in the correct manner, the scheme is unable to accurately preserve the constants in the advection test case. The numerical errors are small for the advection test case, but they appear to be enhanced in the square pulse test case (particularly in the gas density). The MacCormack approach is the only scheme to preserve the constants for the advection test case and does not use the Jacobian. This indicates that the Jacobian matrix may be the cause of the numerical error, but there appears to be little evidence to support this.

We have also illustrated that for the regime of interest, the assumption of an isentropic gas phase is valid since (with the exception of the spurious numerical oscillations in the gas density) the results obtained with the gas energy equation (Model AEE) were in agreement with the isentropic results (Model A).

Acknowledgements

The first author would like to thank the **E**ngineering and **P**hysical **S**cience **R**esearch **C**ouncil for their funding.

A The Primitive Form of Model A-EE

We now reduce each equation of Model AEE into primitive form:

1. Equation (2.1), we can obtain

$$\rho_g(\epsilon_g)_t + \epsilon_g(\rho_g)_t + \epsilon_g\rho_g(u_g)_x + \epsilon_g u_g(\rho_g)_x + \rho_g u_g(\epsilon_g)_x = 0$$

$$\Rightarrow \quad -\rho_g(\epsilon_s)_t + \epsilon_g(\rho_g)_t + \epsilon_g\rho_g(u_g)_x + \epsilon_g u_g(\rho_g)_x - \rho_g u_g(\epsilon_s)_x = 0$$

and by using (2.4),

$$\rho_g(\epsilon_s u_s)_x + \epsilon_g(\rho_g)_t + \epsilon_g\rho_g(u_g)_x + \epsilon_g u_g(\rho_g)_x - \rho_g u_g(\epsilon_s)_x = 0$$

$$\Rightarrow \quad \rho_g\epsilon_s(u_s)_x + \rho_g u_s(\epsilon_s)_x + \epsilon_g(\rho_g)_t + \epsilon_g u_g(\rho_g)_x + \epsilon_g\rho_g(u_g)_x - \rho_g u_g(\epsilon_s)_x = 0.$$

Thus,

$$(\rho_g)_t + u_g(\rho_g)_x + \rho_g(u_g)_x + \frac{\rho_g}{\epsilon_g}(u_s - u_g)(\epsilon_s)_x + \frac{\rho_g}{\epsilon_g}\epsilon_s(u_s)_x = 0.$$

2. Equation (2.2), we can obtain

$$\epsilon_g\rho_g(u_g)_t + u_g(\epsilon_g\rho_g)_t + \epsilon_g\rho_g u_g(u_g)_x + u_g(\epsilon_g\rho_g u_g)_x + \epsilon_g(p_g)_x = -\beta(u_g - u_s)$$

and by using (2.1),

$$\epsilon_g\rho_g(u_g)_t - u_g(\epsilon_g\rho_g u_g)_x + \epsilon_g\rho_g u_g(u_g)_x + u_g(\epsilon_g\rho_g u_g)_x + \epsilon_g(p_g)_x = -\beta(u_g - u_s)$$

$$\Rightarrow \quad \epsilon_g\rho_g(u_g)_t + \epsilon_g\rho_g u_g(u_g)_x + \epsilon_g(p_g)_x = -\beta(u_g - u_s).$$

Thus,

$$(u_g)_t + u_g(u_g)_x + \frac{1}{\rho_g}(p_g)_x = -\frac{\beta}{\epsilon_g\rho_g}(u_g - u_s).$$

3. Equation (2.3)

$$\left(\frac{\epsilon_g p_g}{\gamma - 1} + \frac{1}{2}\epsilon_g\rho_g u_g^2\right)_t + \left(\epsilon_g u_g\left(p_g + \frac{p_g}{\gamma - 1} + \frac{1}{2}\rho_g u_g^2\right)\right)_x + p_g(\epsilon_s u_s)_x = -\beta u_g(u_g - u_s)$$

$$\Rightarrow \quad \frac{1}{\gamma - 1}(\epsilon_g p_g)_t + \frac{1}{2}(\epsilon_g\rho_g u_g^2)_t + \left(\epsilon_g u_g\left(\frac{\gamma p_g}{\gamma - 1} + \frac{1}{2}\rho_g u_g^2\right)\right)_x + p_g(\epsilon_s u_s)_x = -\beta u_g(u_g - u_s)$$

$$\Rightarrow \quad \frac{1}{\gamma - 1}(\epsilon_g p_g)_t + \frac{1}{2}u_g^2(\epsilon_g\rho_g)_t + \epsilon_g\rho_g u_g(u_g)_t + \frac{\gamma}{\gamma - 1}(\epsilon_g u_g p_g)_x + \frac{1}{2}(\epsilon_g\rho_g u_g^3)_x + p_g(\epsilon_s u_s)_x = -\beta u_g(u_g - u_s)$$

using (2.1)

$$\Rightarrow \quad \frac{1}{\gamma - 1}(\epsilon_g p_g)_t - \frac{1}{2}u_g^2(\epsilon_g\rho_g u_g)_x + \epsilon_g\rho_g u_g(u_g)_t + \frac{\gamma}{\gamma - 1}(\epsilon_g u_g p_g)_x + \frac{1}{2}u_g^2(\epsilon_g\rho_g u_g)_x + \epsilon_g\rho_g u_g^2(u_g)_x + p_g(\epsilon_s u_s)_x = -\beta u_g(u_g - u_s)$$

using (2.2)

$$\Rightarrow \quad \frac{1}{\gamma-1}(\epsilon_g p_g)_t + \epsilon_g \rho_g u_g \left(-u_g(u_g)_x - \frac{1}{\rho_g}(p_g)_x - \frac{\beta}{\epsilon_g \rho_g}(u_g - u_s)\right)$$
$$+ \frac{\gamma}{\gamma-1}(\epsilon_g u_g p_g)_x + \epsilon_g \rho_g u_g^2 (u_g)_x + p_g(\epsilon_s u_s)_x = -\beta u_g(u_g - u_s)$$

$$\Rightarrow \quad \frac{1}{\gamma-1}(\epsilon_g p_g)_t - \epsilon_g u_g (p_g)_x - \beta u_g(u_g - u_s)$$
$$+ \frac{\gamma}{\gamma-1}(\epsilon_g u_g p_g)_x + p_g(\epsilon_s u_s)_x = -\beta u_g(u_g - u_s)$$

$$\Rightarrow \quad \frac{1}{\gamma-1}(\epsilon_g p_g)_t - \epsilon_g u_g (p_g)_x + \frac{\gamma}{\gamma-1}\left(\epsilon_g u_g (p_g)_x + p_g(\epsilon_g u_g)_x\right) + p_g(\epsilon_s u_s)_x = 0$$

$$\Rightarrow \quad \frac{1}{\gamma-1}(\epsilon_g p_g)_t + \frac{1}{\gamma-1}\epsilon_g u_g (p_g)_x + \frac{\gamma}{\gamma-1} p_g(\epsilon_g u_g)_x + p_g(\epsilon_s u_s)_x = 0$$

$$\Rightarrow \quad -p_g(\epsilon_s)_t + \epsilon_g (p_g)_t + \epsilon_g u_g (p_g)_x + \gamma p_g(\epsilon_g u_g)_x + (\gamma-1) p_g(\epsilon_s u_s)_x = 0$$

and by using (2.4),

$$\Rightarrow \quad p_g(\epsilon_s u_s)_x + \epsilon_g (p_g)_t + \epsilon_g u_g (p_g)_x + \gamma p_g(\epsilon_g u_g)_x + (\gamma-1) p_g(\epsilon_s u_s)_x = 0$$

$$\Rightarrow \epsilon_g (p_g)_t + \epsilon_g u_g (p_g)_x + \gamma p_g((\epsilon_g u_g)_x + (\epsilon_s u_s)_x) = 0$$

$$\Rightarrow \epsilon_g (p_g)_t + \epsilon_g u_g (p_g)_x + \gamma p_g(\epsilon_g (u_g)_x + u_g(\epsilon_g)_x + \epsilon_s (u_s)_x + u_s(\epsilon_s)_x) = 0$$

$$\Rightarrow \epsilon_g (p_g)_t + \gamma p_g \epsilon_g (u_g)_x + \epsilon_g u_g (p_g)_x + \gamma p_g (u_s - u_g)(\epsilon_s)_x + \gamma p_g \epsilon_s (u_s)_x = 0$$

Hence,

$$(p_g)_t + \gamma p_g (u_g)_x + u_g (p_g)_x + \frac{\gamma p_g}{\epsilon_g}(u_s - u_g)(\epsilon_s)_x + \frac{\gamma p_g \epsilon_s}{\epsilon_g}(u_s)_x = 0.$$

4. Equation (2.4), we can obtain

$$(\epsilon_s)_t + u_s(\epsilon_s)_x + \epsilon_s (u_s)_x = 0.$$

5. Equation (2.5), we can obtain

$$\epsilon_s (u_s)_t + u_s(\epsilon_s)_t + \epsilon_s u_s (u_s)_x + u_s(\epsilon_s u_s)_x + \frac{\epsilon_s}{\rho_s}(p_g)_x + \frac{1}{\rho_s}(p_s)_x = \frac{\beta}{\rho_s}(u_g - u_s)$$

and by using (2.4),

$$\epsilon_s (u_s)_t - u_s(\epsilon_s u_s)_x + \epsilon_s u_s (u_s)_x + u_s(\epsilon_s u_s)_x + \frac{\epsilon_s}{\rho_s}(p_g)_x + \frac{1}{\rho_s}(p_s)_x = \frac{\beta}{\rho_s}(u_g - u_s)$$

$$\Rightarrow \quad \epsilon_s(u_s)_t + \epsilon_s u_s(u_s)_x + \frac{\epsilon_s}{\rho_s}(p_g)_x + \frac{1}{\rho_s}(p_s)_x = \frac{\beta}{\rho_s}(u_g - u_s).$$

Using

$$c_s^2 = \frac{\partial p_s}{\partial \epsilon_s} = \rho_s T_s \quad \text{and} \quad c_T^2 = \frac{\partial p_s}{\partial T_s} = \rho_s \epsilon_s, \tag{A.1}$$

gives

$$\Rightarrow \quad \epsilon_s(u_s)_t + \epsilon_s u_s(u_s)_x + \frac{\epsilon_s}{\rho_s}(p_g)_x + T_s(\epsilon_s)_x + \epsilon_s(T_s)_x = \frac{\beta}{\rho_s}(u_g - u_s).$$

Thus,

$$(u_s)_t + \frac{1}{\rho_s}(p_g)_x + \frac{T_s}{\epsilon_s}(\epsilon_s)_x + u_s(u_s)_x + (T_s)_x = \frac{\beta}{\epsilon_s \rho_s}(u_g - u_s).$$

6. Equation (2.6), we can obtain

$$\epsilon_s(T_s)_t + T_s(\epsilon_s)_t + \epsilon_s u_s(T_s)_x + T_s(\epsilon_s u_s)_x + \frac{2}{3\rho_s}p_s(u_s)_x = -2\beta T_s \rho_s^{-1}$$

and by using (2.5),

$$\epsilon_s(T_s)_t - T_s(\epsilon_s u_s)_x + \epsilon_s u_s(T_s)_x + T_s(\epsilon_s u_s)_x + \frac{2}{3\rho_s}p_s(u_s)_x = -2\beta T_s \rho_s^{-1}$$

$$\Rightarrow \quad \epsilon_s(T_s)_t + \epsilon_s u_s(T_s)_x + \frac{2}{3\rho_s}p_s(u_s)_x = -2\beta T_s \rho_s^{-1}.$$

Thus,

$$(T_s)_t + \frac{2p_s}{3\rho_s \epsilon_s}(u_s)_x + u_s(T_s)_x = -\frac{2\beta}{\rho_s \epsilon_s}T_s.$$

Hence, we obtain the primitive form,

$$\mathbf{w}_t + \mathbf{A}\mathbf{w}_x = \mathbf{R},$$

where

$$\mathbf{w} = \begin{bmatrix} \rho_g \\ u_g \\ p_g \\ \epsilon_s \\ u_s \\ T_s \end{bmatrix}, \quad \mathbf{R} = \begin{bmatrix} 0 \\ -\frac{\beta}{\epsilon_g \rho_g}(u_g - u_s) \\ -\frac{(\gamma-1)\beta}{\epsilon_g}(u_g - u_s)^2 \\ 0 \\ \frac{\beta}{\rho_s \epsilon_s}(u_g - u_s) \\ -\frac{2\beta}{\rho_s \epsilon_s}T_s \end{bmatrix},$$

and

$$\mathbf{A} = \begin{bmatrix} u_g & \rho_g & 0 & \frac{\rho_g}{\epsilon_g}(u_s - u_g) & \frac{\rho_g \epsilon_s}{\epsilon_g} & 0 \\ 0 & u_g & \rho_g^{-1} & 0 & 0 & 0 \\ 0 & \gamma p_g & u_g & \frac{\gamma p_g}{\epsilon_g}(u_s - u_g) & \frac{\gamma p_g \epsilon_s}{\epsilon_g} & 0 \\ 0 & 0 & 0 & u_s & \epsilon_s & 0 \\ 0 & 0 & {\rho_s}^{-1} & \frac{T_s}{\epsilon_s} & u_s & 1 \\ 0 & 0 & 0 & 0 & \frac{2}{3}T_s & u_s \end{bmatrix}.$$

References

[1] A. Bermúdez & M. E. Vázquez, Upwind Methods for Hyperbolic Conservation Laws with Source Terms, *Computers and Fluids* **Vol. 23 No. 8**, 1049 - 1071 (1994).

[2] A. Boemer, H. Qi & U. Renz, Eulerian Simulation of Bubble Formation at a Jet in a Two-Dimensional Fluidized Bed, *Int. J. Multiphase Flow* **Vol. 23 No. 5**, 927 - 944 (1997).

[3] J. Ding & D. Gidaspow, A Bubbling Fluidization Model Using Kinetic Theory of Granular Flow, *AIChE J.* **Vol. 36 No. 4**, 523 - 538 (1990).

[4] A. Harten, High Resolution Schemes for Conservation Laws, *J. Comput. Phys.* **49**, 357 - 393 (1983).

[5] M.E. Hubbard & P. Garcia-Navarro, Flux Difference Splitting and the Balancing of Source Terms and Flux Gradients, *J. Comput. Phys.* **165**, 89 - 125 (2000).

[6] J. Hudson, Numerical Techniques for Morphodynamic Modelling, PhD Thesis, *University of Reading*, October 2001. A colour postscript version of this thesis can be obtained at www.rdg.ac.uk/maths.

[7] J. Hudson & D. Harris, Numerical Modelling of Eulerian Two-Phase Gas-Solid Flow, *MIMS EPrint* **2006.10**, *Manchester Institute for Mathematical Sciences, The University of Manchester, UK*, January 2006.

[8] R. Jackson, The Mechanics of Fluidized Beds. I: the Stability of the State of Uniform Fluidization, *Trans. Inst. Chem. Eng.* **41**, 13 - 21 (1963).

[9] R.J. LeVeque, Balancing Source Terms and Flux Gradients in High-Resolution Godunov Methods: The Quasi-Steady Wave Propagation Algorithm, *J. Comput. Phys.* **146**, 346 - 365 (1998).

[10] R. J. LeVeque, *Finite Volume Methods for Hyperbolic Problems*, Cambridge Tezts In Applied Mathematics, ISBN 0 521 00924 3 (2002).

[11] R.J. LeVeque & H.C. Yee, A Study of Numerical Methods for Hyperbolic Conservation Laws with Stiff Source Terms, *J. Comput. Phys.* **86**, 187 - 210 (1990).

[12] R.W. Lyczkowski, Transient Propagation Behavior of Two-Phase Flow Equations, *AIChE Symp. Ser.* **75** (174), 165 - 174 (1978).

[13] P.L. Roe, Approximate Riemann Solvers, Parameter Vectors and Difference Schemes, *J. Comput. Phys.* **43**, 357 - 372 (1981).

[14] G.A. Sod, A Survey of Several Finite Difference Methods for Systems of Nonlinear Hyperbolic Conservation Laws, *J. Comput. Phys.* **27**, 1 - 31 (1978).

[15] P.K. Sweby, High Resolution Schemes Using Flux Limiters for Hyperbolic Conservation Laws, *SIAM J. Num. Anal.* **21**, 995 (1984).

[16] E.F. Toro, *NUMERICA, a Library of Source Codes for Teaching, Research and Applications*, Numeritek Limited (1999).